

University of Windsor

Scholarship at UWindor

Electronic Theses and Dissertations

Theses, Dissertations, and Major Papers

7-17-1969

Influence of the slenderness and b/t ratios on the inelastic local buckling of angles.

P. S. Mangat
University of Windsor

Follow this and additional works at: <https://scholar.uwindsor.ca/etd>

Recommended Citation

Mangat, P. S., "Influence of the slenderness and b/t ratios on the inelastic local buckling of angles." (1969). *Electronic Theses and Dissertations*. 6574.
<https://scholar.uwindsor.ca/etd/6574>

This online database contains the full-text of PhD dissertations and Masters' theses of University of Windsor students from 1954 forward. These documents are made available for personal study and research purposes only, in accordance with the Canadian Copyright Act and the Creative Commons license—CC BY-NC-ND (Attribution, Non-Commercial, No Derivative Works). Under this license, works must always be attributed to the copyright holder (original author), cannot be used for any commercial purposes, and may not be altered. Any other use would require the permission of the copyright holder. Students may inquire about withdrawing their dissertation and/or thesis from this database. For additional inquiries, please contact the repository administrator via email (scholarship@uwindsor.ca) or by telephone at 519-253-3000ext. 3208.

INFORMATION TO USERS

This manuscript has been reproduced from the microfilm master. UMI films the text directly from the original or copy submitted. Thus, some thesis and dissertation copies are in typewriter face, while others may be from any type of computer printer.

The quality of this reproduction is dependent upon the quality of the copy submitted. Broken or indistinct print, colored or poor quality illustrations and photographs, print bleedthrough, substandard margins, and improper alignment can adversely affect reproduction.

In the unlikely event that the author did not send UMI a complete manuscript and there are missing pages, these will be noted. Also, if unauthorized copyright material had to be removed, a note will indicate the deletion.

Oversize materials (e.g., maps, drawings, charts) are reproduced by sectioning the original, beginning at the upper left-hand corner and continuing from left to right in equal sections with small overlaps.

ProQuest Information and Learning
300 North Zeeb Road, Ann Arbor, MI 48106-1346 USA
800-521-0600

UMI[®]

INFLUENCE OF THE SLENDERNESS AND b/t RATIOS
ON THE INELASTIC LOCAL BUCKLING OF ANGLES

A THESIS

Submitted to the Faculty of Graduate Studies in Partial
Fulfillment of the Requirements for the Degree
of Master of Applied Science in Civil
Engineering from the Univer-
sity of Windsor.

by

P.S.MANGAT

B.Sc., (Civil Eng.), University of London.

Windsor, Ontario, Canada

February, 1969

UMI Number:EC52757

UMI[®]

UMI Microform EC52757
Copyright 2007 by ProQuest Information and Learning Company.
All rights reserved. This microform edition is protected against
unauthorized copying under Title 17, United States Code.

ProQuest Information and Learning Company
789 East Eisenhower Parkway
P.O. Box 1346
Ann Arbor, MI 48106-1346

ABG 7892

APPROVED BY:

J. Kennedy

J. Page

G. Abdul-Sayed

234219

ABSTRACT

An experimental study of inelastic buckling of single and double angle struts was made to obtain information for design. The angles tested were fabricated as regular production work, and their end conditions (hinged and fixed) were chosen to simulate the conditions as they are found in practice. The range of b/t ratios of angles considered in this investigation was between 10.67 and 18.67 inclusive. This range was chosen to establish the bifurcation between inelastic Euler buckling and local buckling, since for a specified slenderness ratio, the mode of failure was known to be:

inelastic Euler buckling when $b/t < 10.67$, and

inelastic local buckling when $b/t > 18.67$.

All angles were 4 feet long and had equal legs. For the purpose of obtaining a statistical average of the buckling stress, three specimens were tested for any one particular b/t ratio and end condition. Such specimens were obtained from one length of angle, together with a stub column from which a stress-strain curve for the material was obtained.

The tests revealed that single angles with $b/t \leq 16$ failed according to Euler buckling theory; the value of the tangent modulus, E_t , at the experimental buckling stress was obtained from the stress-strain curve of the corresponding stub column. The

theoretical buckling stress was then calculated using the Euler buckling formula:

$$\sigma_e = \frac{\pi^2 E_t}{(kl/r)^2}$$

A linear relationship between the slenderness ratio, l/r , and the ratio of the experimental critical stress to yield stress, $\frac{\sigma_{cr}}{\sigma_y}$, was found.

For single angles with $16 < b/t \leq 18.67$, failure was due to local buckling. The theoretical buckling load was calculated using the secant modulus, E_s , in the following plate buckling formula:

$$\sigma_p = \frac{\pi^2 E_s}{12(1-\nu^2)} \left(\frac{t}{b}\right)^2 k$$

A comparison between the theoretical and experimental results for both Euler and local buckling showed good agreement.

The double angles were made by bolting together two single angles, placed back to back, at their mid-length. A gap of 1/4in. was left between the angles in order to facilitate their connection to the gusset plates at the ends. The double angles with $b/t > 10.67$ failed due to local buckling; the values of E_s were found, as before, from the stub column results. These values together with the experimental buckling stress were then substituted in the theoretical plate buckling formula to obtain the values of the plate buckling coefficient k for different b/t ratios. A linear

relationship between b/t and k was found from a regression analysis. The double angle with $b/t = 10.67$ which appears to buckle due to Euler buckling, also satisfies this relationship for the hinged end condition. However, for the fixed end case, this relationship holds only for angles with $b/t > 10.67$.

In order to study the effect of connecting bolts on their strength, double angles with no connecting bolts along their length and with three connecting bolts--one at mid-length and one at each quarter point, were tested.

For the hinged end conditions, the maximum buckling load occurred when no connecting bolts were employed and the load decreased for an increasing number of connecting bolts. The minimum load found was approximately 11% less than the maximum. For the fixed end case, the buckling strength increased with increasing number of connecting bolts, the minimum load being about 10% less than the maximum.

ACKNOWLEDGMENTS

The author wishes to express his sincere gratitude to Dr. J.B.Kennedy (Professor and Head of the Civil Engineering Department at the University of Windsor) for his guidance and encouragement during this study. The author is also deeply obliged to Mr. W.G.Mitchell (Chief Designer of the Canadian Bridge Company) for his valueable help in the construction of the experimental apparatus and supplying the test specimens.

The author is indebted to the Canadian Institute of Steel Construction for sponsering and financing this project and to the Civil Engineering Department of the University of Windsor for the use of the Structural laboratory and its competant staff.

TABLE OF CONTENTS

| | |
|---|------|
| ABSTRACT | iii |
| ACKNOWLEDGEMENTS | vi |
| LIST OF FIGURES | ix |
| LIST OF TABLES | xi |
| LIST OF PHOTOGRAPHS | xii |
| NOMENCLATURE | xiii |
| 1.0 INTRODUCTION | 1 |
| 1.1 Description and the Object of the Investigation | 1 |
| 1.2 Scope of Future Research | 2 |
| 2.0 THEORETICAL BACKGROUND | 3 |
| 2.1 Inelastic Buckling Analysis | 3 |
| 2.2 Calculation of Plate Coefficient k | 7 |
| 2.3 Calculation of Coefficient of Restraint | 8 |
| 3.0 EXPERIMENTAL APPARATUS AND PROCEDURE | 10 |
| 3.1 General Description | 10 |
| 3.2 Test Specimens | 10 |
| 3.3 Apparatus | 12 |
| 3.4 End Fixtures for Single Angles | 12 |
| 3.4.1. Fixed Ends | 12 |
| 3.4.2. Hinged Ends | 14 |
| 3.5 End Fixtures for Double Angles | 15 |
| 3.5.1. Fixed Ends | 15 |
| 3.5.2. Hinged Ends | 16 |
| 3.6 Test Procedure | 16 |
| 3.7 Stub Column Tests | 18 |
| 4.0 ANALYSIS AND DISCUSSION OF EXPERIMENTAL RESULTS | 20 |
| 4.1 General Procedure | 20 |

viii Contents

| | | |
|-------|--|----|
| 4.2 | Single Angles | 21 |
| 4.2.1 | Hinged Ends | 21 |
| 4.2.2 | Fixed Ends | 22 |
| 4.3 | Double Angles | 23 |
| 4.3.1 | Hinged Ends | 23 |
| 4.3.2 | Fixed ends | 24 |
| 5.0 | CONCLUSIONS AND DESIGN RECOMMENDATIONS | 27 |
| 5.1 | Conclusions | 27 |
| 5.2 | Design Recommendations | 28 |
| | BIBLIOGRAPHY | 30 |

LIST OF FIGURES

| Figure | | Page |
|--------|--|------|
| D1. | a. Sketch showing a Restraining and Buckled plate. | 32 |
| | b. Details of a Channel Section. | 32 |
| 1. | a. Single Angles with Fixed End Condition. | 33 |
| | b. Single Angles with Hinged End Condition. | 33 |
| 2. | a. Double Angle Struts with Fixed End Condition. | 34 |
| | b. Double Angle Struts with Hinged End Condition. | 34 |
| 3. | a. Single Angle Specimens for the Hinged End Condition | 35 |
| | b. Single Angle Specimens for the Fixed End Condition. | 37 |
| | c. Double Angle Specimens for the Hinged End Conditions. | 40 |
| | d. Double Angle Specimens for the Fixed End Condition. | 42 |
| 4. | Detailed Drawing of the Apparatus. | 43 |
| 5. | Buckling load obtained by Top-of-the-Knee Method, for a Single Angle Strut with Hinged ends. | 44 |
| 6. | Buckling load obtained by Top-of-the-Knee Method, for a Single Angle Strut with Fixed Ends. | 45 |
| 7. | Buckling load obtained by Top-of-the-Knee Method, for a Double Angle strut with Hinged Ends. | 46 |
| 8. | Buckling load obtained by Top-of-the-Knee Method, for a Double Angle strut with Fixed Ends. | 47 |

x List of Figures.

| Figure | | Page |
|--------|--|------|
| 9. | Typical Stress-Strain curve of a Stub Column | 48 |
| 10. | Euler buckling of Single Angle Struts with Hinged Ends. | 49 |
| D11. | Buckled form of a Single Angle due to Euler buckling. | 50 |
| 11. | Euler buckling of Single Angle Struts with Fixed Ends. | 51 |
| 12. | Variation of Plate Coefficient k with b/t ratios of Double Angle Struts - when tested for Hinged End Conditions. | 52 |
| D13. | Buckled form of a Double Angle Strut. | 50 |
| 13. | Variation of Plate Coefficient k with b/t ratios of Double Angle Struts - when tested for Fixed End Conditions. | 53 |

LIST OF TABLES

| Table | | Page |
|-------|---|------|
| 1. | Results of Tests made on Single Angles with Hinged Ends. | 54 |
| 2. | Results of Tests made on Single Angles with Fixed Ends. | 55 |
| 3. | Results of Tests made on Double Angles with Hinged Ends. | 56 |
| 4. | Results of Tests made on Double Angles with Fixed Ends. | 57 |
| 5. | Results of Tests made on Double Angles with Varying number of Connecting Bolts. | 58 |
| 6. | Details of Members shown in Fig.4. | 59 |

LIST OF PHOTOGRAPHS

| Photograph | Page |
|---|------|
| 1. a. Lay-out of Test apparatus | 60 |
| b. Datran Strain Reader. | 60 |
| 2. Views of the loading arrangement | 61 |
| 3. a. View of 'load cell end' with batten plate removed. | 62 |
| b. View of 'load cell end' with batten plate in position. | 62 |
| 4. View of Load Cell | 63 |
| 5. Hinged End arrangement at the 'load cell end' | 64 |
| 6. Views of the two hinged ends | 65 |
| 7. "End connections for Single Angles" | 66 |
| 8. a. Set-up before commencing a test | 67 |
| b. View after the experiment | 67 |
| 9. Stub Column Test | 68 |
| 10. Buckled forms of Single Angles due to Euler buckling | 69 |
| 11. Buckled forms of Single Angles due to Local buckling | 70 |
| 12. Buckled forms of Double Angles (with no connecting bolts) - Local buckling | 71 |
| 13. Buckled forms of Double Angles (with one connecting bolt) - Local buckling | 72 |
| 14. Buckled forms of Double Angles (with three connecting bolts)-Local buckling | 73 |

NOMENCLATURE

| | |
|------------|---|
| a | Length of plate. |
| b | Width of plate. |
| C_o, C_p | Slenderness ratios defining the Inelastic buckling range of struts. |
| D | Flexural rigidity of a plate. |
| E | Young's Modulus. |
| E_t | Tangent Modulus. |
| E_s | Secant Modulus. |
| e_i | Effective strain. |
| K | Euler buckling constant. |
| k | Plate buckling constant. |
| l | Length of strut. |
| M_x | Moment about xx axis. |
| M_y | Moment about yy axis. |
| M_{xy} | Twisting moment. |
| n | Numerical factor. |
| P_{cr} | Experimental critical buckling load. |
| r | Numerical factor. |
| t, t_c | Thickness. |
| v | Plasticity function. |
| w | Displacement in z direction. |

xiv Nomenclature

| | |
|----------------------------------|--|
| x, y, z | Rectangular co-ordinates. |
| ϵ_x, ϵ_y | Strains in x and y directions respectively. |
| $\phi, \bar{\phi}$ | Angles of rotation due to buckling. |
| γ | Unit shearing strain. |
| κ | A function of E_t and E_s . |
| η | A function of E_t , E_s , and E . |
| ν | Poisson's ratio. |
| ρ_1, ρ_2 | Radii of curvature in x and y directions respectively. |
| ρ_3 | Angle of twist. |
| $\bar{\sigma}_x, \bar{\sigma}_y$ | Stresses in x and y directions respectively. |
| σ_e | Theoretical Euler buckling stress. |
| σ_p | Theoretical plate buckling stress. |
| σ_{cr} | Experimental buckling stress. |
| σ_i | Equivalent tensile stress. |
| σ_y | Yield stress at 0.01% offset. |
| τ | Ratio of E_t to E . |
| τ_{xy} | Shear strain along yy axis, perpendicular to xx axis. |
| ζ | Coefficient of Restraint. |
| $\bar{\zeta}$ | Function of coefficient of Restraint. |

CHAPTER 1

INTRODUCTION

1.1. Description and the object of the investigation.

A study of the inelastic buckling of single and double angle struts is made to obtain information for design purposes. The range of b/t ratios of angles considered in this investigation is between 10.67 and 18.67 inclusive. The type of failure obtained for this range of b/t ratios includes both Euler buckling and local buckling. One of the aims of this study is to establish the bifurcation between the inelastic Euler buckling and the local buckling* since for the same slenderness ratios used herein the mode of failure is known to be: inelastic Euler buckling for angles with $b/t < 10.67$ and inelastic local buckling for $b/t > 18.67$. The angles tested and their end conditions (hinged and fixed) are chosen to simulate such structural elements as they are found in practice. Buckling of struts in the inelastic range is analysed using the theories of Ilyushin and Stowell.^{2,3} These theories provide constants which when substituted

* Euler and local buckling of struts is clearly separated and no transition exists between the two modes of buckling. See Ref:1

in place of Young's modulus in the elastic buckling equations, give formulae that are valid for inelastic buckling.

The Euler and local buckling theory applicable to single angles, in the elastic range, is generally known.^{4,5} A theoretical analysis of double angles for local buckling, however, is not possible since the restraining effect of the bolted legs on the free legs or on each other cannot be defined. Hence it becomes desirable to carry out experiments in order to obtain empirical formulae for design. In the case of single angles a comparison is made between the experimental and theoretical results.

1.2. Scope of future Research.

Double angles with b/t ratios different from those investigated here may be tested to obtain buckling formulae for them. Studies can also be made on double angles which are formed by joining together single angles in ways different from those used in this investigation. This work can be further extended to angles of unequal legs. The effect of lateral loads or torsional moments, in addition to axial load, may also be studied for both single and double angles.

CHAPTER 2

THEORETICAL BACKGROUND

2.1 Inelastic buckling analysis.

Stowell² analysed inelastic buckling by basing it on Shanley's conception⁶ that in a compression member loaded in the plastic range, buckling proceeds simultaneously with increasing axial load, so that no strain reversal occurs. Stowell takes Poisson's ratio, ν as 0.5, but the effect of any error of ν is largely eliminated by the following computational device: the buckling stress for elastic buckling must be multiplied by η * to give the critical stress for the plastic case. The values of η are, therefore, obtained by dividing the critical buckling stress in the plastic range by the critical stress found for elastic buckling, but with $\nu=0.5$. Hence the ratio η is only slightly affected by the error in ν .

Experiments on metals⁷ have shown that initial yielding and subsequent plastic flow are not affected by a moderate hydrostatic compression or tension either applied alone or superimposed on a

* Values of η , calculated by Stowell's theory for certain type of plates, are given in Ref.5 on page 353.

state of combined stresses. The plastic yield conditions are, therefore, defined by the hypothesis of Huber, Mises, and Hencky, which implies isotropy of the material in the plastic range. This theory assumes that the energy of shear distortion at failure due to combined stresses equals the value of the energy of shear distortion for simple tension. Applying this hypothesis, the equivalent tensile stress σ_i , producing the same effective strain e_i as the combined stresses $\bar{\sigma}_x, \bar{\sigma}_y, \tau_{xy}$ in a two dimensional stress system is found to be:

$$\sigma_i = \sqrt{\bar{\sigma}_x^2 + \bar{\sigma}_y^2 - \bar{\sigma}_x \bar{\sigma}_y + 3 \tau_{xy}^2} \quad (1)$$

Assuming isotropy of the material in the inelastic range, and for the loading condition,

$$\sigma_i = v(e_i) ; \text{ where } v \text{ is the plasticity function.}$$

It follows that $\sigma_i/e_i = E_s$ and $d\sigma_i/de_i = E_t$, where E_s and E_t are the secant and tangent modulus respectively.

For the isotropic material, the following relations are valid:

$$\frac{\bar{\sigma}_x - \nu \bar{\sigma}_y}{\epsilon_x} = \frac{\sigma_i}{e_i} = \frac{v(e_i)}{e_i} ; \quad \frac{\bar{\sigma}_y - \nu \bar{\sigma}_x}{\epsilon_y} = \frac{\sigma_i}{e_i} = \frac{v(e_i)}{e_i} \quad (2a)$$

where ϵ_x and ϵ_y are the strains in x and y directions respectively and ν is the Poisson's ratio for the material.

$$\text{Also, } \frac{2(1+\nu) \tau_{xy}}{\gamma} = \frac{\sigma_i}{e_i} = \frac{v(e_i)}{e_i} \quad (2b)$$

$$\text{Using } \nu = 1/2 \text{ and putting } S_x = \bar{\sigma}_x - \bar{\sigma}_y/2 ; S_y = \bar{\sigma}_y - \bar{\sigma}_x/2 ;$$

$$\text{gives } \epsilon_x = S_x/E_s ; \epsilon_y = S_y/E_s ; \gamma = 3\tau_{xy}/E_s \quad (3)$$

$$\text{and } \bar{\sigma}_x = 4/3 (S_x + S_y/2) ; \bar{\sigma}_y = 4/3 (S_y + S_x/2) ; \tau_{xy} = E_s \gamma/3. \quad (4)$$

Assuming small deflections, the increments in strains in any direction are proportional to their respective increments in curvature.

$$\text{Therefore, } \delta \epsilon_x = -z \delta \rho_1 ; \delta \epsilon_y = -z \delta \rho_2 ; \delta \gamma = 2z \delta \rho_3. \quad (5)$$

Differentiating the equation $S_x = \epsilon_x E_s$, gives:

$$\delta S_x = E_s \delta \epsilon_x - \frac{\epsilon_x}{e_i} \left(\frac{\sigma_i}{e_i} - \frac{d\sigma_i}{de_i} \right) \delta e_i \quad (6)$$

The work done by the internal forces when the strut buckles is:

$$\begin{aligned} \sigma_i \delta e_i &= \bar{\sigma}_x \delta \epsilon_x + \bar{\sigma}_y \delta \epsilon_y + \tau_{xy} \delta \gamma \\ \therefore \delta e_i &= -\frac{z}{\sigma_i} (\bar{\sigma}_x \delta \rho_1 + \bar{\sigma}_y \delta \rho_2 + 2\tau_{xy} \delta \rho_3) \end{aligned}$$

Substituting in (6) and simplifying,

$$\delta S_x = -E_s z \delta \rho_1 + \frac{\epsilon_x}{\sigma_i} (E_s - E_t) z (\bar{\sigma}_x \delta \rho_1 + \bar{\sigma}_y \delta \rho_2 + 2\tau_{xy} \delta \rho_3) \quad (7)$$

Similarly, δS_y and $\delta \tau_{xy}$ may be calculated.

Now,

$$\begin{aligned} \delta M_x &= \int_{-t/2}^{t/2} \delta \bar{\sigma}_x z dz. \\ \therefore \delta M_x &= -D' \left[\left(1 - \frac{3}{4} k \frac{\bar{\sigma}_x^2}{\sigma_i^2}\right) \delta \rho_1 + \frac{1}{2} \left(1 - \frac{3}{2} k \frac{\bar{\sigma}_x \bar{\sigma}_y}{\sigma_i^2}\right) \delta \rho_2 - \frac{3}{2} k \frac{\bar{\sigma}_x \tau_{xy}}{\sigma_i^2} \delta \rho_3 \right] \quad (8) \end{aligned}$$

$$\text{where } D' = E_s t^3/9 \quad \text{and } k = 1 - E_t/E_s \quad (9)$$

Similarly,

$$\delta M_y = -D' \left[\left(1 - \frac{3}{4} k \frac{\bar{\sigma}_y^2}{\sigma_i^2}\right) \delta \rho_2 + \frac{1}{2} \left(1 - \frac{3}{2} k \frac{\bar{\sigma}_x \bar{\sigma}_y}{\sigma_i^2}\right) \delta \rho_1 - \frac{3}{2} k \frac{\bar{\sigma}_y \tau_{xy}}{\sigma_i^2} \delta \rho_3 \right] \quad (10)$$

and

$$\delta M_{xy} = -\frac{D'}{2} \left[\left(1 - \kappa \frac{3\tau_{xy}^2}{\sigma_i^2}\right) \delta \rho_3 - \frac{\kappa}{2} \left(\frac{\sigma_x \tau_{xy}}{\sigma_i^2} \delta \rho_1 + \frac{\sigma_y \tau_{xy}}{\sigma_i^2} \delta \rho_2 \right) \right] \quad (11)$$

Taking w as the deflection of the plate perpendicular to the plane of the plate,

$$\delta \rho_1 = \frac{\partial^2 w}{\partial x^2}; \quad \delta \rho_2 = \frac{\partial^2 w}{\partial y^2}; \quad \delta \rho_3 = \frac{\partial^2 w}{\partial x \partial y} \quad (12)$$

For the condition $\sigma_x = \tau_{xy} = 0$ and hence $\sigma_i = \sigma_x$, we obtain

from the general plate buckling equation:

$$D' \left[\left(1 - \frac{\kappa}{4}\right) \frac{\partial^4 w}{\partial x^4} + 2 \frac{\partial^4 w}{\partial x^2 \partial y^2} + \frac{\partial^4 w}{\partial y^4} \right] + t \sigma_x \frac{\partial^2 w}{\partial x^2} = 0 \quad (13)$$

The solution to this equation for various boundary conditions gives a value for the factor η which, when substituted in the elastic buckling equation, makes the relation suitable for inelastic failure.

The general equation for local buckling, therefore, is:

$$\sigma_p = \frac{\pi^2 \eta E}{12(1-\nu^2)} \left(\frac{t}{b}\right)^2 k \quad (14)$$

For elastic buckling, $\eta = 1$.

For columns failing in the inelastic range due to Euler buckling,

$$\eta = E_t/E.$$

For inelastic local buckling of a long flange, one unloaded end

simply supported, $\eta = E_s/E$.

The above two cases of η cover the struts tested in this investigation.

2.2 Calculation of plate coefficient k.

A suitable method for determining the value of local buckling constant k is given in Reference 5. A coefficient of restraint, ζ , is introduced in this method. This is a dimensionless number which is a function of the dimensions of the buckled and restraining plates.

At the edge where the restraining and buckled plates meet, the following boundary conditions apply (see fig D1) :

$$\phi = \bar{\phi}$$

Assuming that M_y (moment per unit length) is proportional to $\bar{\phi}$. Therefore, $M_y = -\bar{\zeta}\bar{\phi}$, where $\bar{\zeta} = \text{constant}$.

A relation obtained from plate theory gives^{4,8}:

$$M_y = -D \left[\frac{\partial^2 w}{\partial y^2} + \nu \frac{\partial^2 w}{\partial x^2} \right] \text{ at } y = b/2 \quad (15)$$

$$\text{and } \phi = \pm \left(\frac{\partial w}{\partial y} \right)_{y=b/2} \quad (16)$$

Since $\phi = \bar{\phi}$, therefore $\pm \left(\frac{\partial w}{\partial y} \right)_{y=b/2} = - \frac{M_y}{\bar{\zeta}}$

Hence,

$$\left\{ \frac{D}{\bar{\zeta}} \left[\frac{\partial^2 w}{\partial y^2} + \nu \frac{\partial^2 w}{\partial x^2} \right] \pm \frac{\partial w}{\partial y} \right\}_{y=b/2} = 0$$

Putting $\bar{\zeta} = \frac{2}{b} \frac{D}{\zeta}$, gives (17)

$$\left[\frac{\partial w}{\partial y} \pm \frac{b}{2} \zeta \left(\frac{\partial^2 w}{\partial y^2} + \nu \frac{\partial^2 w}{\partial x^2} \right) \right]_{y=b/2} = 0 \quad (18)$$

From plate theory, we know that w can be assumed to be a function of $\sin\left(\frac{n\pi x}{a}\right)$. Using the above boundary condition obtained

by equating δ and $\bar{\delta}$, and also applying the other boundary conditions known, the equation for w is solved. The solution provides the general equation 14, for local buckling which includes the constant k . The value of k , for various sections, is given in Ref. 5.

Each leg of an equal-legged angle is treated as a plate and is considered to be free on one unloaded edge and hinged on the common edge of the two legs. The value of k for this condition is 0.425.

2.3 Calculation of coefficient of Restraint.

To calculate the coefficient of restraint, ζ , the deflection \bar{w} of the restraining plate is obtained in terms of M_y , from the general plate theory. This is differentiated to obtain the value of $\bar{\delta}$, as follows:

$$\bar{\delta} = \left(\frac{\partial \bar{w}}{\partial y} \right)_{y=b/2} = A (M_y)$$

The value of A depends on the dimensions of a specimen, the buckle wave-length, and η .

Substituting $M_y = -\left(\frac{2}{b} \frac{D}{\zeta}\right) \bar{\phi}$, gives,

$$\bar{\delta} = -A \left(\frac{2}{b} \frac{D}{\zeta}\right) \bar{\phi}$$

Therefore,

$$\zeta = -A \frac{2}{b} D \quad (19)$$

This value of ζ is only due to the moment produced at the edge of the restraining and buckled plates. The effect of longitudinal stress is taken into account by multiplying these values

of ζ by a factor \bar{F} . This factor is determined in a way such that it becomes infinite if the buckled plate and the restraining plate, considered as simply-supported plates at their non-free ends, buckle at the same stress.

As an example, consider a channel section with its flange as the restraining plate, as shown in figure D1. Considering the web to be hinged at both ends and using the appropriate value of k for this case, the buckling stress for the web is calculated. This stress is equated to the buckling stress of the flange which is considered as hinged on one end and free on the other. Hence, it gives:

$$4(t/b)^2 = 0.425(t_c/c)^2$$

$$\text{Therefore, } 9.4t_c^2/b^2t_c^2 = 1$$

$$\text{Hence, } \bar{F} = 1/(1-9.4t_c^2/b^2t_c^2) \quad (20)$$

$$\text{and } \zeta = -2AD\bar{F}/b \quad (21)$$

The angles that buckle as columns can be analysed using the Euler buckling formula:

$$\sigma_e = \frac{\pi^2 \eta \cdot E}{(kl/r)^2} \quad (22)$$

$$\text{where } \eta = \frac{Et}{E}$$

CHAPTER 3

EXPERIMENTAL APPARATUS AND PROCEDURE

3.1 General Description.

The setting-up of the experiment involved:

(a) The design of test specimens.

Single and double angle struts with b/t ratios between 10.67 and 18.67 were designed to have slenderness ratios such that they would buckle in the inelastic range of stress.

(b) The design of a Test rig.

The testing apparatus was designed to suit the dimensions of the angles. Hinged and fixed end conditions for the specimens were also designed.

3.2 Test Specimens.

All angles were 4 feet long and had equal legs (nine single angles tested with hinged ends were 4ft.3-1/2in. long). Although smaller lengths of angles could have been tested more conveniently in a standard loading machine, this was avoided since local effects due to end conditions are more marked on smaller

lengths of specimens.⁹ All angles with leg width ≥ 3 in. were of G 40.12 steel while smaller angles were of A 36 steel. The Elastic moduli and the yield stresses for the two steels are similar.

To ensure inelastic buckling, the slenderness ratios of the angles were kept within the range of Intermediate columns. This range was found by using the following relationship.¹⁰

$$C_0 < Kl/r \leq C_p \quad (23)$$

The values of C_0 and C_p used here were 20 and 90 respectively.

For the purpose of obtaining a statistical average of the buckling stress, three specimens were tested for any one particular b/t ratio and end condition. Such specimens were obtained from one length of angle, together with a stub column. The specimens and the stub columns were milled at the ends. Suitable holes were punched at the ends to enable bolting of the angles to "end connections", as shown in figs. 1 and 2.

The double angle struts were made by bolting together two single angles, placed back to back, at their mid-length by means of a 5/8 in. diameter bolt. A gap of 1/4 in. was kept between the angles in order to facilitate their connection to the gusset plates at the ends. A set of three double angle struts each connected together along its length by means of three bolts- one at mid-length and one at each quarter point, and a set of three double angles with no connecting bolts along its length, were made.

The details of all the angle specimens are given in figs. 3 a,b,c,d.

3.3 Apparatus.

A detailed drawing of the apparatus used for the tests on the angles is shown in fig.4. It comprises of two 9ft.7-1/2in. long channels, placed back to back - 1ft. 2in. apart - and bolted on to a 8ft.4in. X 20in. X 1/4in. plate at the bottom as shown in the drawing of Main Frame A1 in fig. 4. The connections at the ends are a system of channel and angle sections and these are shown in sections AA and BB of fig. 4.

The test frame was placed on stools, in a horizontal position and it was made level. The compression tests were carried out inside the frame. A hydraulic jack, with a capacity of 120 kips., was used to load the struts. The load readings were obtained by using a 100 kips. capacity Universal Flat load cell which was connected to a Budd Datran Digital Strain Recorder. At any particular load the strain in the load cell was measured by the Datran Recorder. This strain was converted into its corresponding load by using the calibration curve (graph of the load versus strain reading) of the load cell.

3.4 End fixtures for Single Angles.

3.4.1 Fixed Ends.

An arrangement used for testing single angles for fixed

end conditions is shown in fig. 1(a). Slider A was placed adjacent to the hydraulic jack. Details of the slider are given by "Guide B1" in fig. 4. A slider was comprised of two 1-1/2 in. thick plates of high strength steel, which were welded to the two ends of a 9 in. long I-section. A conical hole on one of the faces of the slider was used to obtain a hinge joint as explained in section 3.4.2. later. For the fixed end case, one of the "end connections for single angles" was bolted on to the front face of slider A. Details of this "end connection" are given in fig. 4. It consists of a 1-1/2 in. thick plate of high strength steel to which two 5in. X 3-1/2in. X 3/8in. angles were bolted.- these angles facilitated the connection of single angle specimens to the "end connection".

The slider arrangement was adjusted so that its centre line coincided with the centre line of the test frame. Any gap between the slider edges and the frame walls was shimmed precisely, without causing a tight fit, so that no rocking of the slider could occur, and at the same time frictional resistance was small. Friction was further minimised by lubricating the contact surfaces of the slider and frame walls. The gap between the top of the slider and the channels of the frame was shimmed precisely and lubricated. A channel-section batten plate was bolted on top of the slider to guide its motion.

Slider B, with "end connections for single angles" bolted on it, was placed in the same way as slider A, at the far end of

the frame, as shown in fig. 1(a). Any gaps were shimmed as before, with a channel-section batten plate bolted on top.

The calibrated load cell was placed centrally at the far end of the frame, beyond slider B. Load was transmitted to the load cell through a 1-1/2in. diameter steel ball which rested in a semi-circular hole in the load cell.

The single angle, tested for fixed end conditions, was placed between the "end connections" on sliders A and B. Between each leg of the test specimen and a protruding leg of the angles on the "end connections" a suitable thickness of shims was placed in order to bring the centroid of the specimen in line with the point of application of load, thus ensuring concentric loading of the strut. The test angles were bolted onto the protruding legs of angles on the "end connection" by means of 5/8in. diameter bolts.

Details of shims used in the experiments are shown in fig. 4.

3.4.2 Hinged ends.

The arrangement used to test single angle struts for hinged end conditions is shown in fig. 1(b). The slider A remains the same as for the fixed end case. The "end connection for single angles" was unbolted from the slider and a spherical ball of chrome steel, 2 in. in diameter, was placed in the conical holes between the slider and the "end connection". "enlarged view C" on fig. 4 gives details

of the holes on the slider and the "end connections".

On the far end, slider B was moved to the end of the frame, with the load cell being shifted forward to form the hinged end for a test specimen. A 2in. diameter chrome steel ball was placed between the load cell and the "end connection". The two angles of each "end connection" were bolted on, and the test specimen was placed between these in the same manner as that for the fixed end case. Suitable shims were provided to ascertain concentric loading.

The channel section batten plate was located on the top of the load cell and suitable packing was inserted in order to ensure that the load cell was fixed in place when the batten plate was bolted on to the test frame. Packing was also fitted tightly between the load cell and the vertical walls of the channels, to avoid any sideways rocking of the load cell.

3.5 End fixtures for Double Angles.

3.5.1 Fixed Ends.

The set-up for fixed ends of double angles is shown in fig.2(a). It is the same as that used for single angles except for the "end connections". The details of an "end connection", used in this case, are shown in fig.4. It comprises of a 1-1/2in. thick, high strength steel plate with a conical hole at the centre of one face. A 1/4in. thick gusset plate was welded to the other face, along its vertical centre axis. The gusset plate had three 11/16in. diameter holes which facilitated the connection of the test specimen to

the gusset plate.

The "end connections for double angles" were then bolted onto sliders A and B as shown in fig.2(a). The double angle specimen was then bolted onto the gusset plate with one angle on either side of the plate, using 5/8in. diameter bolts. The struts with a bolt at their mid-length, were bolted together using a 5/8in. diameter bolt with a 1/4in. thick washer inserted between the angles. A similar procedure was used for struts with holes at the centre and quarter points of the length.

3.5.2 Hinged Ends.

The set-up for double angles with hinged ends is shown in fig.2(b). Slider B was moved to the far end of the frame and the load cell was shifted forward to form the hinged end condition, fixed in position as explained in 3.4.2. A 2in. diameter chrome steel ball was provided between the load cell and the "end connection for double angles" in order to simulate a "pin" joint. A second hinge was obtained by placing a steel ball in the conical holes, between the slider A and an "end connection". A test specimen was then placed in position as explained in 3.5.1.

3.6 Test Procedure.

For both single and double angle tests, a specimen was placed between the "end connections" and by loading the hydraulic jack, slider A was moved forward until the test angle was slightly

compressed. The jack was, then, released. The "end connections", in the case of hinged ends, were made level by means of a spirit level. Wedges were fitted between the base of the test frame and the bottom of the "end connection" in order to avoid any rotation until the test was started. This, however, was unnecessary for the fixed end condition since the "end connections" were fixed in position. The specimen was, then, adjusted until it assumed its correct position, by tapping it lightly with a hammer. Having attained the correct position of the specimen, it was bolted tightly to the "end connection". For the hinged end case, the wedges placed under the "end connections" were removed before testing.

Dial gages, accurate to the nearest 0.001in, were used to obtain the deflections. For single angles, deflections were generally measured at four points - two on each leg. These points were chosen closer to the centre of span where deflections tended to be larger. For double angles, five and sometimes six dial gages were used, distributing them on the three legs of the strut. After a few tests, it was possible to predict the behaviour of the struts with the dial gages placed at suitable points. The bases of the dial gages were fixed on the test frame; and, therefore, the deflections obtained for a specimen were relative to the frame displacements. In a few cases, the displacement of the test frame were measured relative to stationary objects and these were found to be negligible.

The load cell was connected to the Datran Digital Strain

Reader and its zero load reading was established before any load application--this was done before a test specimen was placed in position, since after fitting an angle, a slight compression was always detected.

Before starting the experiment, the dial gages were adjusted to zero. The specimen was then loaded by means of the hydraulic jack. At suitable increments of load, the deflections were read on the dial gages and the load cell reading was noted.

A graph of load versus deflection was plotted for every strut, and its buckling load was found from this graph by using top-of-the-knee method.^{11,12} The critical load, according to this method, is the load corresponding to the top of the knee of a curve of load versus deflection of a strut. Examples of application of this procedure are shown in figs. 5,6,7,8.

3.7 Stub Column Tests.

The Stub Column Tests were carried out to obtain the stress-strain relationship for the steel angles tested. For angles with $b = 3\text{in.}$ or more, the length of the stub column used was 1ft. For angles with smaller leg dimensions, 6in. long stub columns were tested. The stub columns were designed in accordance with Ref. 13. The ends of the columns were milled to ensure axial loading.

To obtain the strains in a stub column, four uni-axial electrical resistance strain gages were mounted on each stub column

- two on each leg. The gages on one leg were placed centrally on each face, opposite to each other. In this manner, any bending stresses in a leg were nullified when a mean of the two gage readings was taken. The stub column test was performed in a Tinius-Olsen hydraulic testing machine in accordance with the procedure in ref. 13. The Datran Digital Strain Reader was used to obtain the strain.

For two stub column tests, one of the strain gages used was bi-axial. This was done to obtain the axial and lateral strains at a point in order to calculate the Poisson's ratio of the material.

CHAPTER 4

ANALYSIS AND DISCUSSION OF EXPERIMENTAL RESULTS

4.1 General Procedure.

Graphs were plotted showing the relationship between deflection and load for various locations on a test angle. The load readings were given by the load cell. Typical such plots are shown in figs. 5,6,7,8. The buckling load of a specimen was found from its load-deflection curves by using the Top-of-the-knee method as mentioned before and explained more fully in Refs. 11,12. Since for each specimen, a number of load-deflection curves were obtained, the buckling load of the specimen was found by using the mean value of the loads read from each curve. For the purpose of obtaining a statistical average of the buckling stress, three specimens were tested for any one particular b/t ratio and end condition.

From the stress-strain graph of the material (obtained from a stub column test), the secant modulus and tangent modulus were found at the experimental buckling stress, for specimens with a particular b/t ratio. A typical Stress-strain graph obtained from a stub column test is shown in fig. 9.

The average value of Poisson's ratio was found to be 0.261.

4.2 Single Angles.

4.2.1 Hinged ends.

The experimental results were analysed to provide design curves for the struts and to enable the comparison of experimental and theoretical results. The theoretical values of the buckling loads were calculated using the theory discussed in Chapter 2.

Having obtained the values of experimental buckling load (P_{cr}), secant modulus (E_s) and tangent modulus (E_t) by using the procedure of section 4.1., these values of E_t and E_s were then substituted in the theoretical expressions for Euler and local buckling, respectively, in order to calculate the theoretical buckling loads. Poisson's ratio in the inelastic range was assumed to be the same as in the elastic range.⁵

The yield stress σ_y (at offset=0.01 per cent) was obtained for specimens of each b/t ratio, from the stress-strain curve of the stub column test. A graph of the ratio of experimental buckling stress to yield stress σ_{cr}/σ_y , versus the strut slenderness ratio l/r , was plotted as shown in fig. 10, for angles with $b/t \leq 16$; a best-fit straight line was drawn through these points by applying the Least Square Method of curve fitting¹⁴. The validity of the linear regression was confirmed by calculating the correlation coefficient of the straight line. Angles with $b/t > 16$ failed due to local buckling and hence did not follow the deduced relationship:

$$\sigma_{cr}/\sigma_y = 1.660 - 0.00911(l/r)$$

of Euler buckling for angles with $b/t \leq 16$. The results of calculati-

ons made for single angles with hinged ends are given in Table 1.

Angles with $b/t \leq 16$, which buckled according to Euler theory, failed by bending about their weakest axis zz , as shown in fig. 11. It can be observed that the apex of the angle bent downwards while both the legs bent inwards towards each other.

For the angles that buckled locally, one of the legs bulged outwards while the other bulged inwards, with the angle between the two legs remaining sensibly constant. The apex remained straight along the length of the angle.

4.2.2 Fixed ends.

The theoretical buckling load of specimens which failed according to Euler theory was calculated in terms of the constant K by using Euler buckling formula (22). This load was then equated to the corresponding experimental buckling load of the strut in order to calculate the constant K . The values of K so obtained for angles with different b/t ratios are shown in Table 2. To estimate the effectiveness of the fixed end conditions used in the present experiments, a comparison was made (see Table 2) between the experimental values of K for angles with different b/t ratios to the K values of ideally fixed and hinged end conditions ($K=1/2$ and $K=1$ respectively for perfectly fixed and hinged ends). The comparison shows that the experimental fixed end conditions are actually closer to those for a hinge than for an ideal fixed end condition, especially for larger

angles with $b > 2$ in. For angles with $b \leq 2$ in., the mean value of K is 0.714 - which suggests that the end condition is in between a hinge and a perfect fixed end.

For the angles with $b/t \leq 16$, which failed according to Euler buckling, a linear relationship was found between their slenderness ratios and the non-dimensional ratio of their experimental buckling stress σ_{CR} , to the corresponding secant modulus E_s . This graph is shown in fig. 11. The ratio E_s/E (where E is the Young's modulus of the material) was also calculated for these angles, as shown in Table 2. It was seen that these ratios were reasonably constant for all cases, and hence their mean value ($E_s/E=0.94$) may be used for design purposes.

The angles with $b/t > 16$ failed due to local buckling. The appearance of the buckled specimens, for local as well as Euler failures, was similar to that explained in section 4.2.1.

4.3 Double Angles.

4.3.1 Hinged ends.

The values of experimental buckling stress σ_{CR} , secant modulus E_s , and tangent modulus E_t were found for angles with each b/t ratio by using the procedure of section 4.1. Substituting for E_s in the plate buckling formula (14), the critical buckling stress was calculated in terms of the plate coefficient k . This stress was then equated to the experimental buckling stress and hence the

values of k were obtained for double angles with different b/t ratios. A graph was plotted between the values of k and the corresponding b/t ratios; and a best fit linear relationship was obtained as shown in fig. 12.

The Euler buckling load of the double angles was also calculated, by substituting for E_t in the Euler formula (22), as shown in Table 3. These theoretical values tend to be higher than the experimental buckling stresses, thus suggesting that Euler buckling is not the mode of failure for these angles.

The buckled forms of the angles with $b/t = 10.67$ showed that the angles failed by bending about the xx axis as shown in fig. D13. No wrinkles appeared on the legs of the double angles.

All angles with $b/t > 10.67$ tended to bend about the xx axis and with simultaneous appearance of local buckling waves on the bolted legs especially near the centre of span where the bolt was situated.

4.3.2 Fixed ends.

The experimental results for double angles with fixed ends were analysed in the same manner as explained in section 4.3.1. The results are presented in Table 4; it can be seen from Tables 3 and 4 that for double angles with $b/t > 10.67$, the buckling loads for fixed and hinged end conditions could be related as follows:

$$(\sigma_{cr})_{\text{fixed ends}} = 1.14 (\sigma_{cr})_{\text{hinged ends}}$$

Compared to angles with higher b/t ratios, the effect of fixed end conditions on angles with $b/t \leq 10.67$ is much more considerable, thus suggesting that Euler buckling occurs for the angles with $b/t \leq 10.67$.

The appearance of the buckled forms showed that double angles with $b/t=10.67$ failed by bending about the xx axis (see fig.D13). The double angles with $b/t > 10.67$ failed due to local buckling and wrinkles were observed on all legs- especially near the centre of span and at the central bolt-connection. As before, a linear relationship between k and b/t was established for this case as shown in fig.13.

In order to study the effect of connecting bolts on their strength, double angles with no connecting bolts along their length and with three connecting bolts- one at mid-length and one at each quarter point, were tested. These tests were made for both fixed and hinged end conditions - one set of three double angles with $b/t=16$ being tested for each end condition. The results obtained from these tests are given in Table 5.

It is known that plate elements usually possess post-buckling strength^{15,16} and a plate after buckling may, in some cases, carry without failure a load many times larger than the critical load at which buckling begins. It is, therefore, desirable to have a knowledge of the post-buckling strength of the members for the

234210

purposes of design. For the experiments conducted on single and double angles, in this study, it was seen that the collapse of the struts occurred soon after the critical buckling stress was reached, thus suggesting that the angles do not possess any post-buckling strength. Thus, a safe design of such angles would be based on their critical buckling stress.

CHAPTER 5

CONCLUSIONS AND DESIGN RECOMMENDATIONS

5.1 Conclusions.

Within the range of the experiments carried out and reported herein, the following conclusions can be made:

(1) Single angles with $b/t \leq 16$, for both hinged and fixed end conditions, fail due to Euler buckling. For angles with $16 < b/t \leq 18.67$, local buckling occurs.

The end fixity provided for single angles is not very effective; the angles with leg width $b > 2$ in. may be taken as pin-ended, with the factor $K=1$, while angles with $b \leq 2$ in. can be treated as partially fixed ended struts with $K=0.714$.

(2) Double angles for hinged and fixed end conditions, with $10.67 < b/t \leq 18.67$, fail due to local buckling. The plate coefficient k varies linearly with b/t ratios of angles.

(3) The strength of fixed-ended double angles with $10.67 < b/t \leq 18.67$ is greater than that for double angles with hinged end conditions by approximately 14%.

The end fixity has a more marked effect on angles with $b/t=10.67$, which suggests that these angles fail due to Euler buckling.

(4) The number of connecting bolts used along the length has no serious effect on the buckling strength of double angles. For the hinged end conditions, the maximum buckling load occurs when no connecting bolts are used and the load decreases with increase in number of bolts. The minimum load is approximately 11% less than the maximum. For the fixed end case, the buckling strength increases with increase in number of connecting bolts, the minimum load being about 10% less than the maximum.

5.2 Design Recommendations.

- (1) It would be conservative to neglect the end fixity of single and double angle struts and to design them as pin-ended members.
- (2) Single angle struts with hinged ends, with $b/t \leq 16$ and $20 \leq Kl/r \leq 96$, can be designed using the deduced relationship given in fig. 10.

Single angle struts with $b/t > 16$ may be designed using the theoretical plate buckling equation (14). The value of E_s in this equation may be taken as:

$$E_s = 0.94 E \quad (\text{See table 1})$$

This relationship is obtained in the same manner as explained in section 4.2.2.

Fixed ended single angles with $b/t \leq 16$ can be designed using the relationship as found in fig. 11. For the type of fixed end connections used in this investigation, Euler constant K is 1

for angles with leg width $b > 2\text{in.}$; for angles with smaller legs,
 $K = 0.714$.

(3) Double angle, hinged end struts with $10.67 \leq b/t \leq 18.67$ may be designed using the relationship as found in fig.12. The constant k can be obtained for a corresponding b/t ratio from the graph of fig.12. Substituting this value of k in the plate buckling equation (14) the critical load for a double angle strut can be found.

(4) The buckling stress of fixed ended double angle struts with $10.67 < b/t \leq 18.67$ is approximately 1.14 times that of the corresponding hinged end double angles. The graph of fig.13 may also be used to obtain values of k for known b/t ratios of double angles; substituting these values of k in the plate buckling equation (14), the critical buckling load of a double angle strut can be found.

For both fixed and hinged ended double angles with $10.67 < b/t \leq 18.67$, a suitable relationship between E_s and E was found, using the procedure explained in section 4.2.2., to be:

$$E_s = 0.965 E \quad (\text{See tables 3 and 4})$$

The values of E_s required in the plate buckling equation (14) can, therefore, be obtained using the above relationship.

BIBLIOGRAPHY

1. Bridget F.J., Jerome C.C., Vosseller A.B., Some New Experiments on Buckling of Thin-Wall Construction, A.S.M.E. Trans., Applied Mechanics Division, Vol. 56, p. 569, 1934.
2. Stowell E.Z., A Unified Theory of Plastic Buckling of Columns and Plates, NACA, Tech. Note 1556, 1948.
3. Ilyushin A.A., The Elasto-plastic Stability of Plates, Translation in NACA Tech. Mem. 1188.
4. Timoshenko S.P., Gere J.M., Theory of Elastic Stability, Second Edition, 1961, McGraw-Hill.
5. Bleich F., Buckling Strength of Metal Structures, 1952, McGraw-Hill.
6. Shanley F.R., Inelastic Column Theory, Journal of Aeronautical Sciences, Vol. 14, No. 5, May 1947.
7. Bridgman P.W., Flow and Fracture, Trans. American Institute of Metallurgical Engineers, Iron and Steel Div., Vol. 162, 1945.
8. Timoshenko S., Woinowsky-Kreiger S., Theory of Plates and Shells, Second Edition, McGraw-Hill.
9. Timoshenko S., Goodier J.N., Theory of Elasticity, Second Edition, 1951, McGraw-Hill.
10. Canadian Institute of Steel Construction, Handbook of Steel Construction, First Edition, Second Printing, December, 1967.
11. Hu P.C., Lundquist E.E., Batdorf S.B., Effect of Small Deviations from Flatness on the Effective Width and Buckling of Plates in Compression, Tech. Note, No. 1124, NACA.

12. Stowell E.Z., Heimerl G.J., Libove C., Lundquist E.E.,
Buckling Stresses for Flat Plates and Sections,
A.S.C.E., Proceedings, Vol. 77, Page 1, July,
1951.
13. Johnston B.G., Guide to Design Criteria for Metal Compression
Members, Column Research Council, Second Edition,
John Wiley and Sons, Inc.
14. Neville A.M., and Kennedy J.B., Basic Statistical Methods for
Engineers and Scientists, International Textbook
Company.
15. Beedle L.S., Blackman J.H., Cooper P.B., Driscoll G.C., Eney
W.J., Errera S.J., Estuar F.R., Fisher J.W.,
Galambus T.V., Hansell W.C., Lay M.G., Levi V.,
Lu L.W., Ostapenko A., Reemsnyder H.S., Rumpf J.L.,
Slutter R.G., Tall L., Yen B.T., Structural
Steel Design, The Ronald Press.
16. George Winter, Light Gage Cold-Formed Steel Design Manual,
1962 Edition, American Iron and Steel Institute.

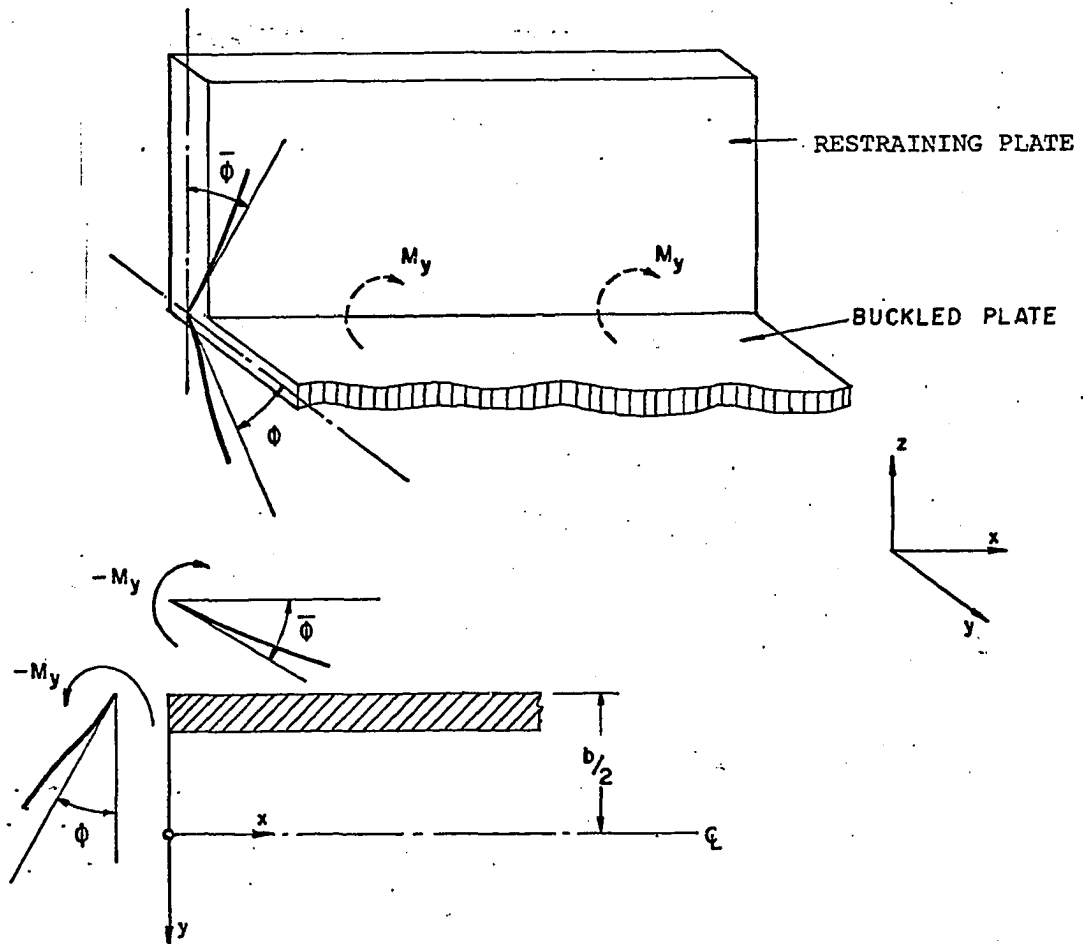


Fig.D1.a. Restraining and Buckled plate of a Section.

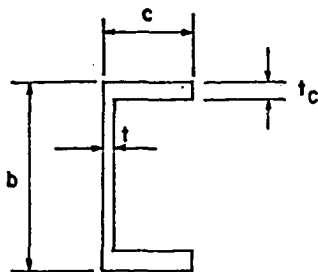
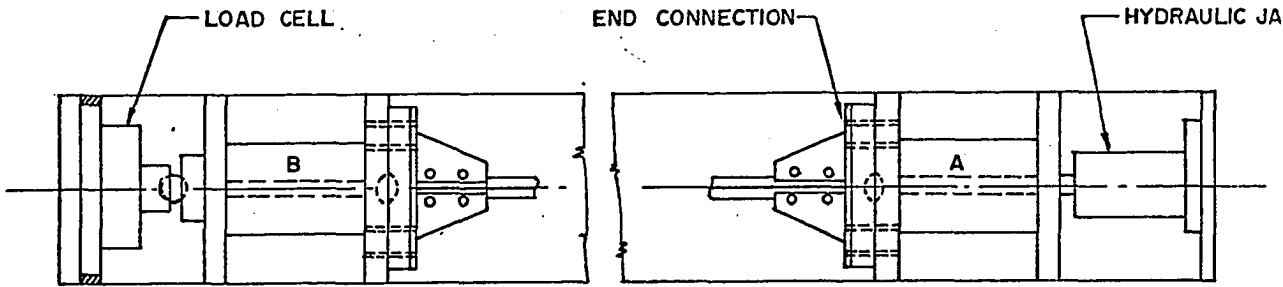
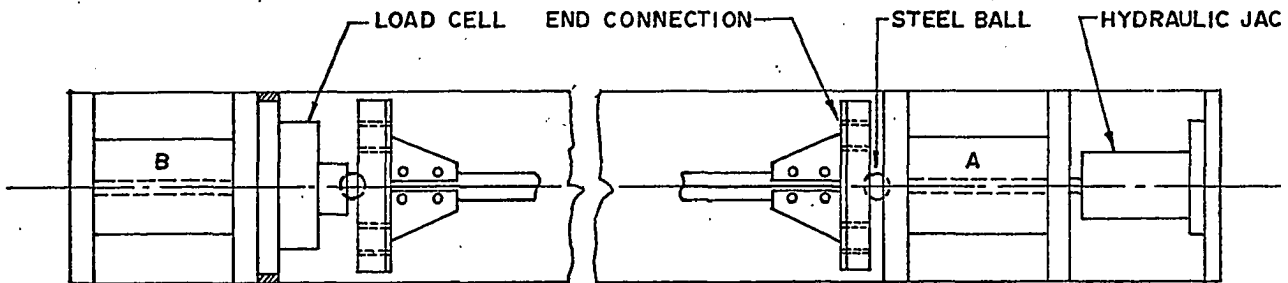


Fig.D1.b. Details of a Channel section.



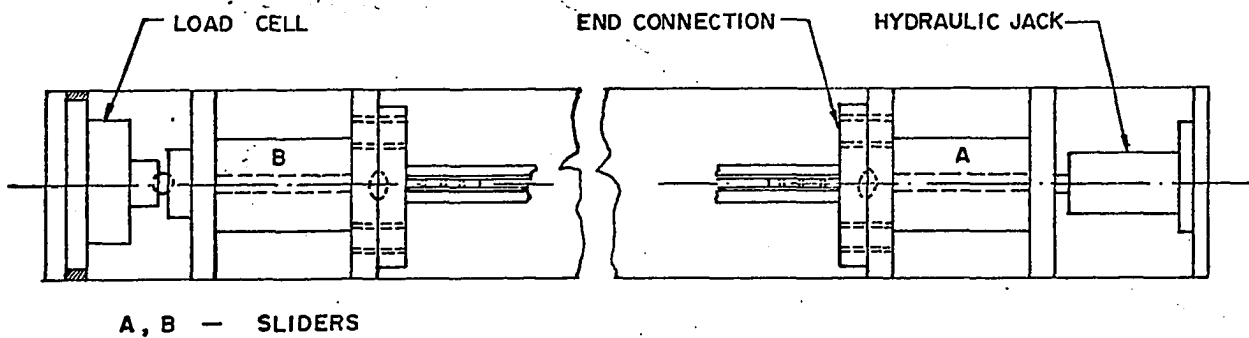
A, B - SLIDERS

(a) SINGLE ANGLES TESTED FOR FIXED END CONDITION

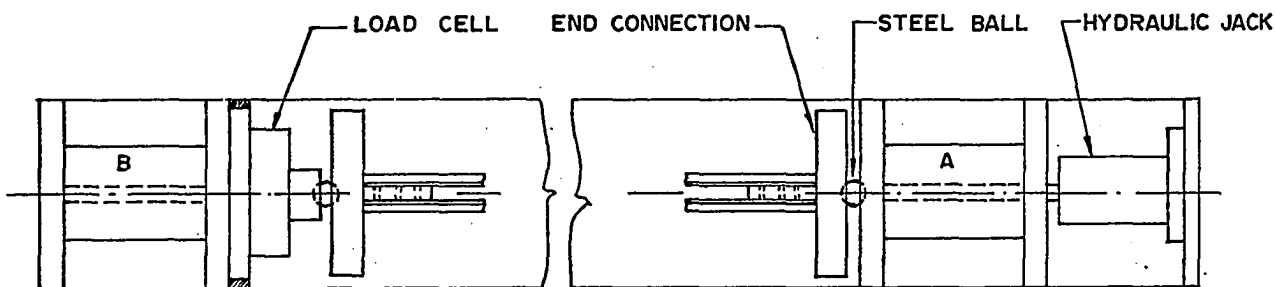


(b) SINGLE ANGLES TESTED FOR HINGED END CONDITION

Fig.1. Experimental Set-up for Single Angles.

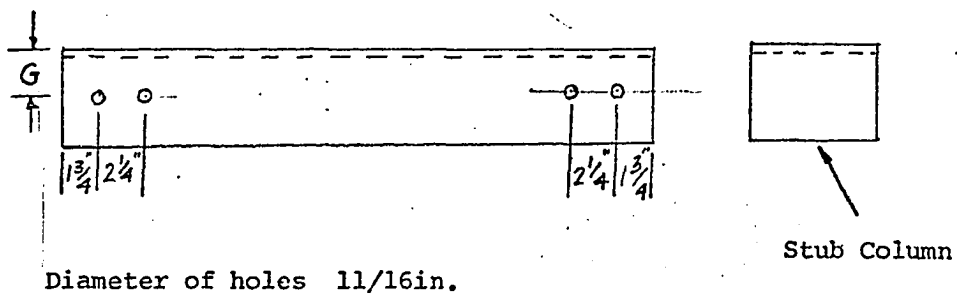


(a) DOUBLE ANGLE STRUTS TESTED FOR FIXED END CONDITION



(b) DOUBLE ANGLE STRUTS TESTED FOR HINGED END CONDITION

Fig.2. Experimental Set-up for Double Angle Struts.

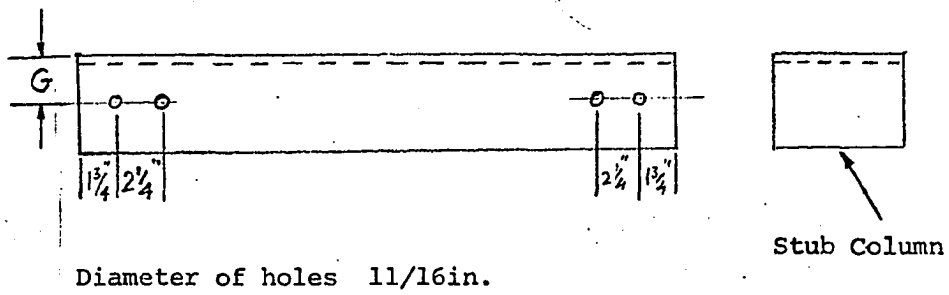


| Section (Inches) | Dimension G (Inches) | Section (Inches) | Dimension G (Inches) |
|---------------------|----------------------------|---------------------|----------------------------|
| 3 x 3 x 3/16 | 1-5/16in. | 3½ x 3½ x 1/4 | 1-15/32in. |
| 3 x 3 x 1/4 | 1-11/32in. | 3½ x 3½ x 5/16 | 1-1/2in. |
| 3½ x 3½ x 3/16 | 1-7/16in. | 4 x 4 x 5/16 | 1-5/8in. |

Fig. 3(a). Single Angle Specimens for the Hinged End Conditions.
(Continued overleaf)

| Quantity | Description | Shape (Inches) | Length | Remarks |
|----------|-------------|--|-------------------------|----------------------------------|
| 3 | Strut | $3\frac{1}{2} \times 3\frac{1}{2} \times 5/16$ | 3ft.8 $\frac{1}{2}$ in. | Cut from same piece of angle. |
| 1 | Stub | $3\frac{1}{2} \times 3\frac{1}{2} \times 5/16$ | 1ft. | |
| 3 | Strut | $3 \times 3 \times 1/4$ | 4ft. | Cut from same piece of angle. |
| 1 | Stub | $3 \times 3 \times 1/4$ | 1ft. | |
| 3 | Strut | $4 \times 4 \times 5/16$ | 3ft.8 $\frac{1}{2}$ in. | Cut from same piece of angle. |
| 1 | Stub | $4 \times 4 \times 5/16$ | 1ft. | |
| 3 | Strut | $3\frac{1}{2} \times 3\frac{1}{2} \times 1/4$ | 3ft.8 $\frac{1}{2}$ in. | Cut from same piece of angle. |
| 1 | Stub | $3\frac{1}{2} \times 3\frac{1}{2} \times 1/4$ | 1ft. | |
| 3 | Strut | $3 \times 3 \times 3/16$ | 3ft.8 $\frac{1}{2}$ in. | Cut from same piece of angle. |
| 1 | Stub | $3 \times 3 \times 3/16$ | 1ft. | |
| 3 | Strut | $3\frac{1}{2} \times 3\frac{1}{2} \times 3/16$ | 4ft. | Cut from same piece of angle. |
| 1 | Stub | $3\frac{1}{2} \times 3\frac{1}{2} \times 3/16$ | 1ft. | |

Fig. 3(a). Single Angle Specimens for the Hinged End Condition.



| Section (Inches) | Dimension G (Inches) | Section (Inches) | Dimension G (Inches) |
|---|----------------------------|--|----------------------------|
| $1\frac{3}{4} \times 1\frac{3}{4} \times 1/8$ | 1in. | $2\frac{1}{2} \times 2\frac{1}{2} \times 3/16$ | 1-3/16in. |
| $2 \times 2 \times 1/8$ | 1-1/16in. | $3 \times 3 \times 1/4$ | 1-11/32in. |
| $2 \times 2 \times 3/16$ | 1-1/16in. | $3\frac{1}{2} \times 3\frac{1}{2} \times 3/16$ | 1-7/16in. |

Fig. 3(b). Single Angle Specimens for the Fixed End Condition.

(Continued overleaf)

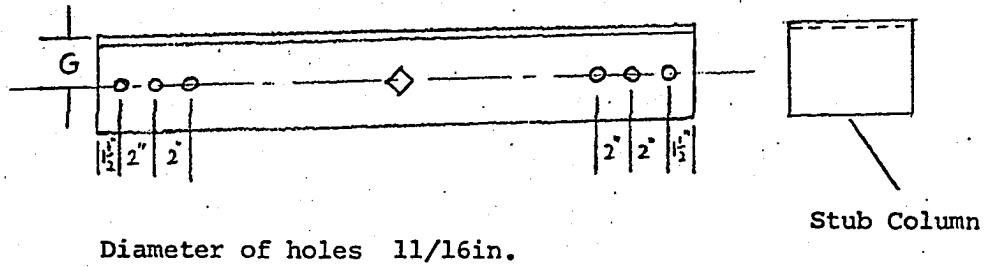
| Quantity | Description | Shape (Inches) | Length | Remarks |
|----------|-------------|-------------------|-----------|----------------------------------|
| 3 | Strut | 2 x 2 x 3/16 | 4ft. | Cut from same piece of angle. |
| 1 | Stub | 2 x 2 x 3/16 | 6in. | |
| 3 | Strut | 3½ x 3½ x 5/16 | 3ft.8½in. | Cut from same piece of angle. |
| 1 | Stub | 3½ x 3½ x 5/16 | 1ft. | |
| 3 | Strut | 2½ x 2½ x 3/16 | 4ft. | Cut from same piece of angle. |
| 1 | Stub | 2½ x 2½ x 3/16 | 6in. | |
| 3 | Strut | 3½ x 3½ x 1/4 | 3ft.8½in. | Cut from same piece of angle. |
| 1 | Stub | 3½ x 3½ x 1/4 | 1ft. | |
| 3 | Strut | 1¾ x 1¾ x 1/8 | 4ft. | Cut from same piece of angle. |
| 1 | Stub | 1¾ x 1¾ x 1/8 | 6in. | |
| 3 | Strut | 3 x 3 x 3/16 | 3ft.8½in. | Cut from same piece of angle. |
| 1 | Stub | 3 x 3 x 3/16 | 1ft. | |

Fig. 3(b). Single Angle Specimens for the Fixed End Condition.

(Continued overleaf)

| Quantity | Description | Shape (Inches) | Length | Remarks |
|----------|-------------|-------------------|-----------|----------------------------------|
| 3 | Strut | 2 x 2 x 1/8 | 4ft. | Cut from same piece of angle. |
| 1 | Stub | 2 x 2 x 1/8 | 6in. | |
| 3 | Strut | 3½ x 3½ x 3/16 | 3ft.8½in. | Cut from same piece of angle. |
| 1 | Stub | 3½ x 3½ x 3/16 | 1ft. | |

Fig. 3(b). Single Angle Specimens for the Fixed End Condition.



| Section (Inches) | Dimension G (Inches) | Section (Inches) | Dimension G (Inches) |
|---|----------------------------|--|----------------------------|
| $1\frac{3}{4} \times 1\frac{3}{4} \times 1/8$ | 1in. | $2\frac{1}{2} \times 2\frac{1}{2} \times 3/16$ | 1-3/16in. |
| $2 \times 2 \times 1/8$ | 1-1/16in. | $3 \times 3 \times 1/4$ | 1-11/32in. |
| $2 \times 2 \times 3/16$ | 1-1/16in. | $3\frac{1}{2} \times 3\frac{1}{2} \times 3/16$ | 1-7/16in. |

Fig. 3(c). Double Angle Specimens for the Hinged End Condition.

(Continued overleaf)

| Quantity | Description | Shape (Inches) | Length | Remarks |
|----------|-------------|-------------------|-----------|----------------------------------|
| 3 | Strut | 3 x 3 x 1/4 | 3ft.8½in. | Cut from same piece of angle. |
| 1 | Stub | 3 x 3 x 1/4 | 1ft. | |
| 3 | Strut | 2 x 2 x 3/16 | 3ft.8½in. | Cut from same piece of angle. |
| 1 | Stub | 2 x 2 x 3/16 | 6in. | |
| 3 | Strut | 2½ x 2½ x 3/16 | 3ft.8½in. | Cut from same piece of angle. |
| 1 | Stub | 2½ x 2½ x 3/16 | 6in. | |
| 3 | Strut | 1¾ x 1¾ x 1/8 | 3ft.8½in. | Cut from same piece of angle. |
| 1 | Stub | 1¾ x 1¾ x 1/8 | 6in. | |
| 3 | Strut | 2 x 2 x 1/8 | 3ft.8½in. | Cut from same piece of angle. |
| 1 | Stub | 2 x 2 x 1/8 | 6in. | |
| 3 | Strut | 3½ x 3½ x 3/16 | 3ft.8½in. | Cut from same piece of angle. |
| 1 | Stub | 3½ x 3½ x 3/16 | 1ft. | |

Fig. 3(c). Double Angle Specimens for the Hinged End Condition.

| Quantity | Description | Shape (Inches) | Length | Remarks |
|----------|-------------|-------------------|--------|----------------------------------|
| 3 | Strut | 2 x 2 x 3/16 | 4ft. | Cut from same piece of angle. |
| 1 | Stub | 2 x 2 x 3/16 | 6in. | |
| 3 | Strut | 3 x 3 x 1/4 | 4ft. | Cut from same piece of angle. |
| 1 | Stub | 3 x 3 x 1/4 | 1ft. | |
| 3 | Strut | 2½ x 2½ x 3/16 | 4ft. | Cut from same piece of angle. |
| 1 | Stub | 2½ x 2½ x 3/16 | 6in. | |
| 3 | Strut | 1¼ x 1¼ x 1/8 | 4ft. | Cut from same piece of angle. |
| 1 | Stub | 1 x 1 x 1/8 | 6in. | |
| 3 | Strut | 2 x 2 x 1/8 | 4ft. | Cut from same piece of angle. |
| 1 | Stub | 2 x 2 x 1/8 | 6in. | |
| 3 | Strut | 3½ x 3½ x 3/16 | 4ft. | Cut from same piece of angle. |
| 1 | Stub | 3½ x 3½ x 3/16 | 1ft. | |

Fig. 3(d). Double Angle Specimens for the Fixed End Condition.

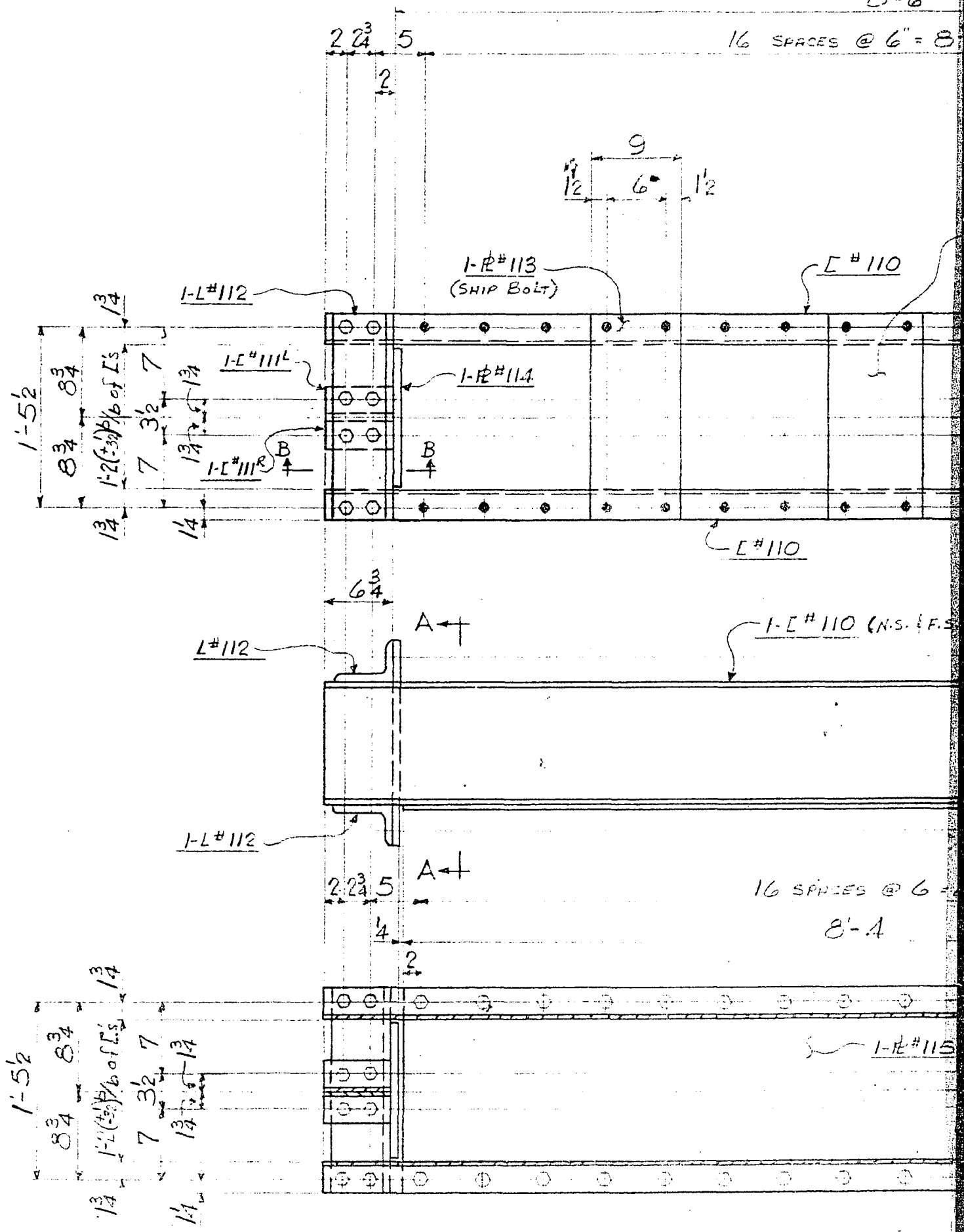
NOTE TO USERS

Oversize maps and charts are microfilmed in sections in the following manner:

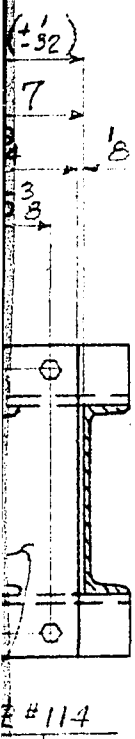
LEFT TO RIGHT, TOP TO BOTTOM, WITH SMALL OVERLAPS

This reproduction is the best copy available.

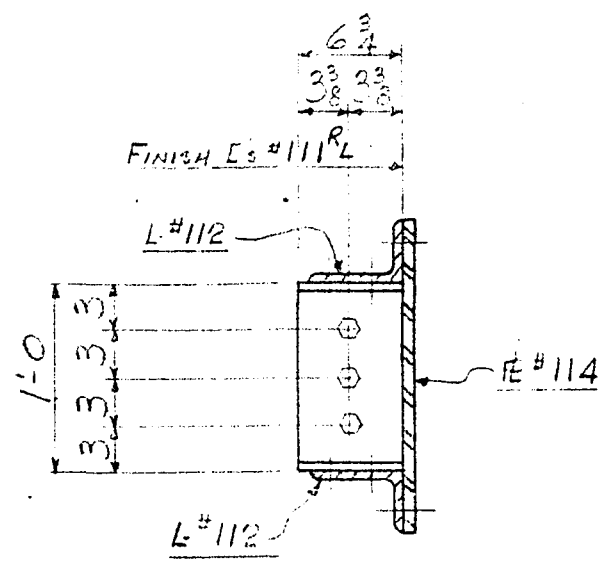
UMI



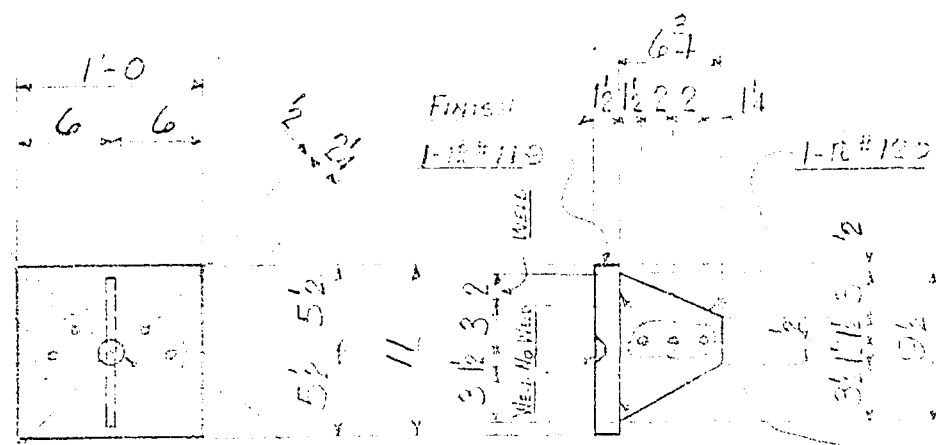
MAIN FRAME A



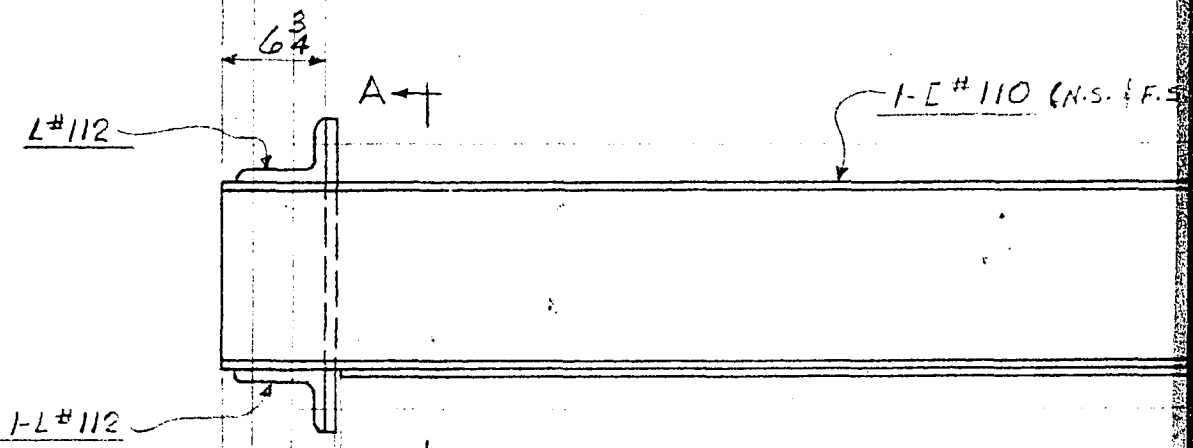
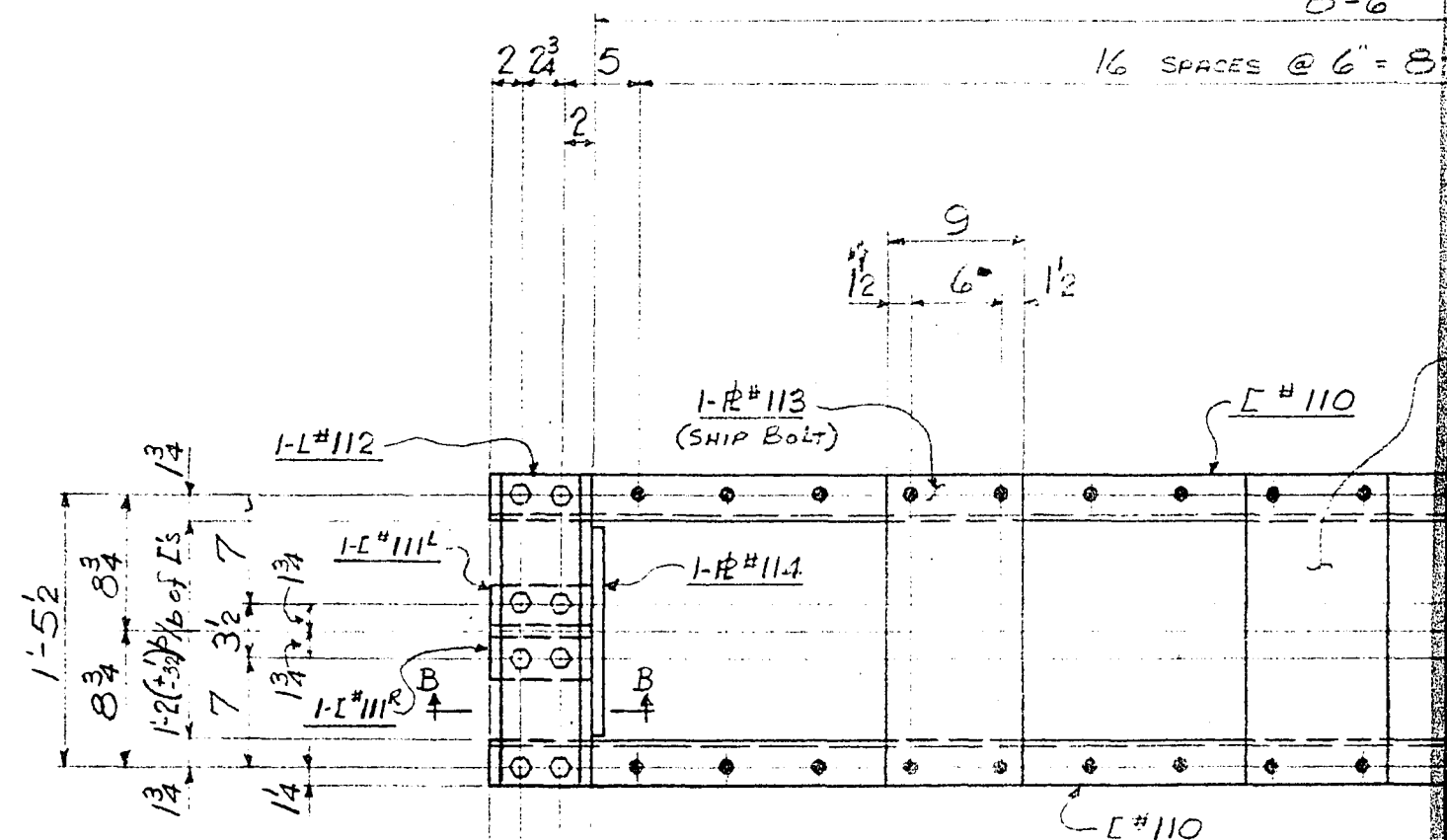
A-A



SECTION B-B

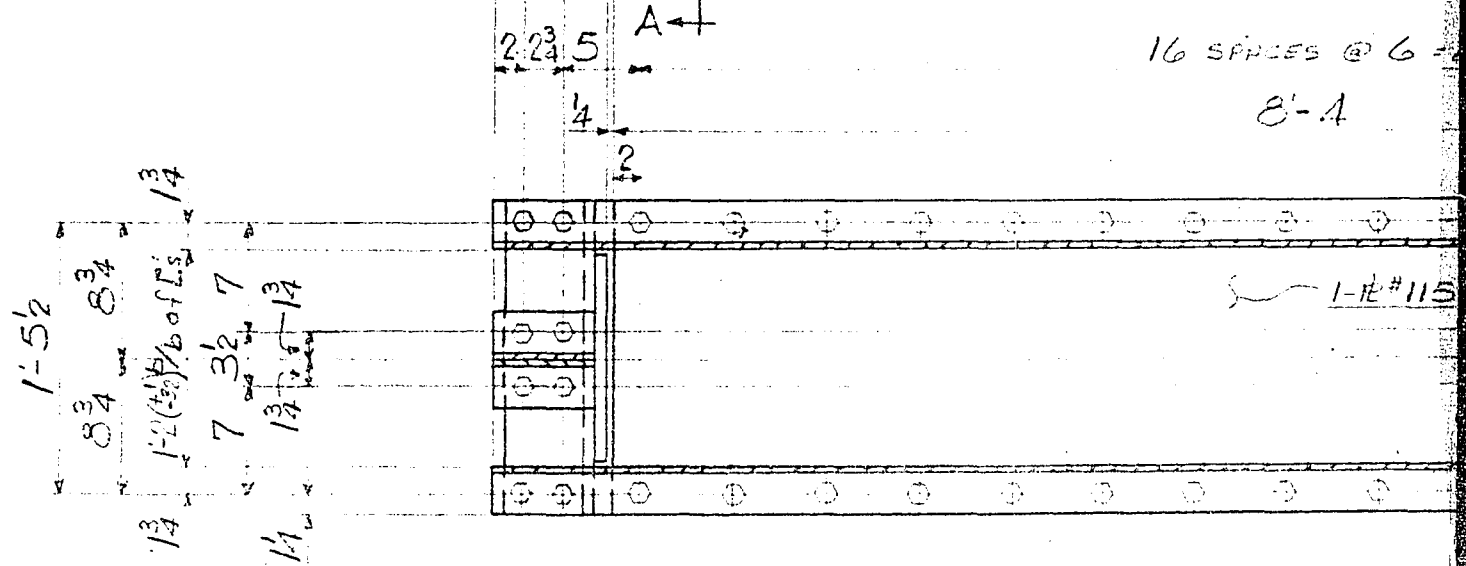


16 SPACES @ 6" = 8'

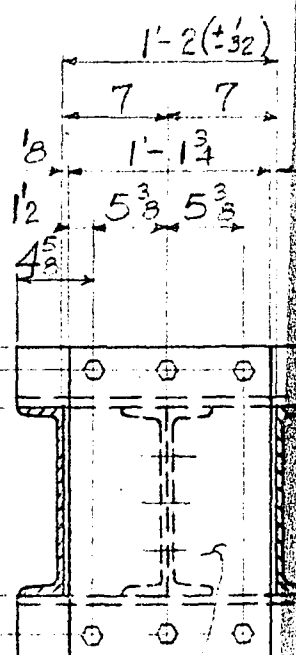
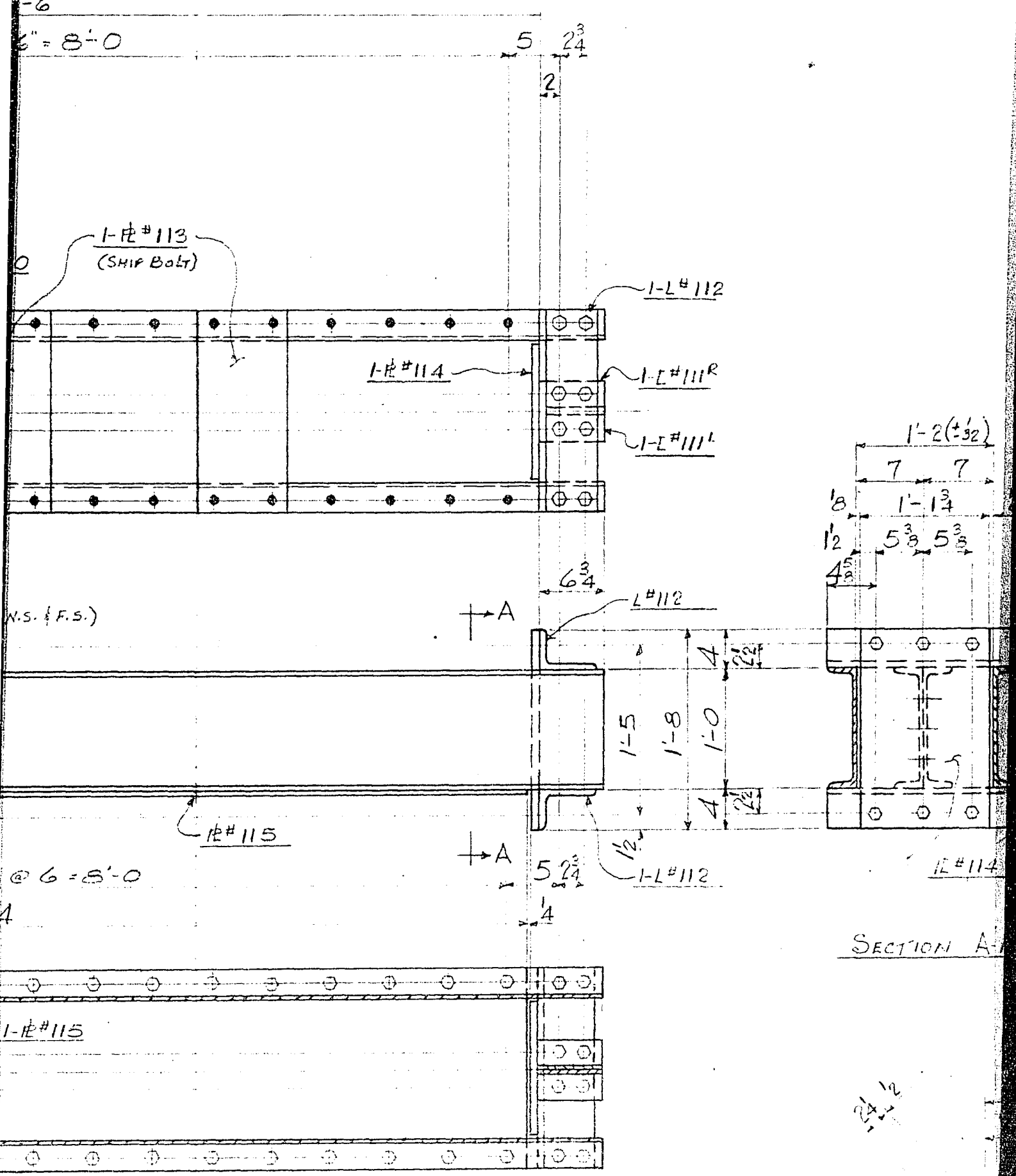


16 SPACES @ 6" = 8'

8'-4



MAIN FRAME A



SECTION A-A

24 1/2

11

FRAME A1

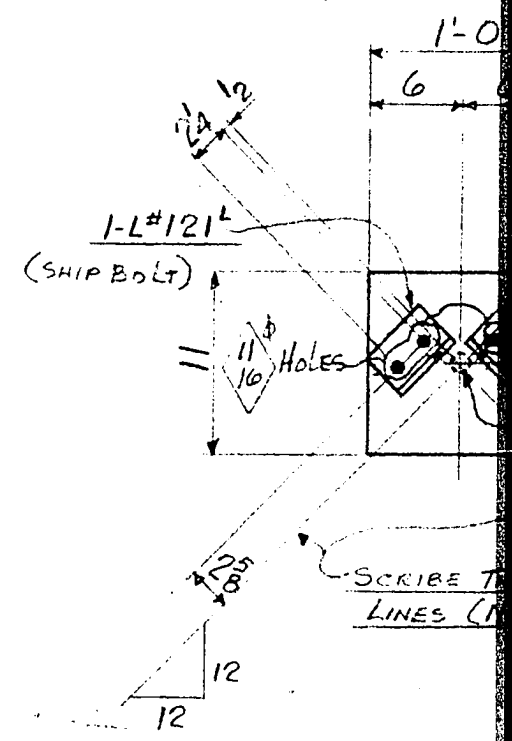
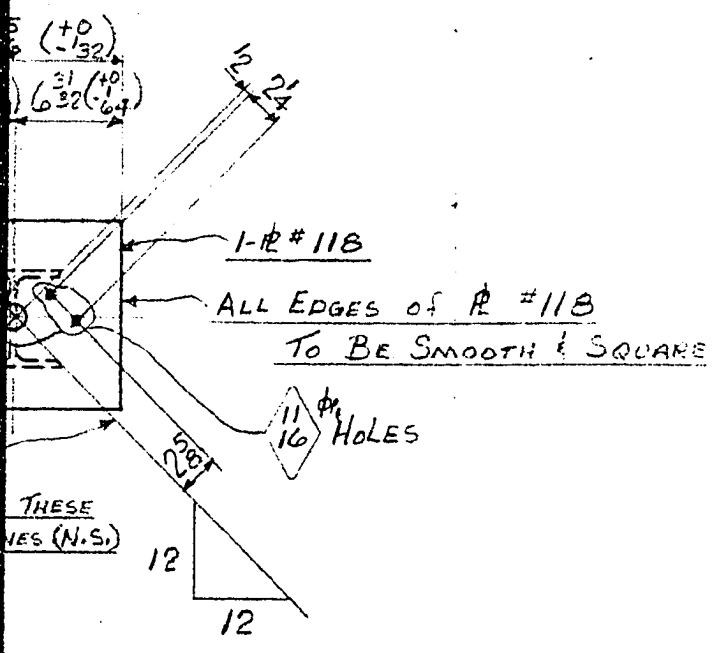
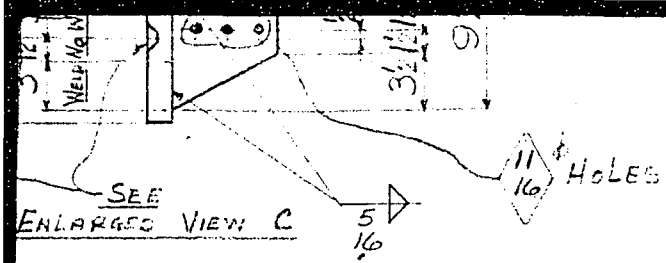
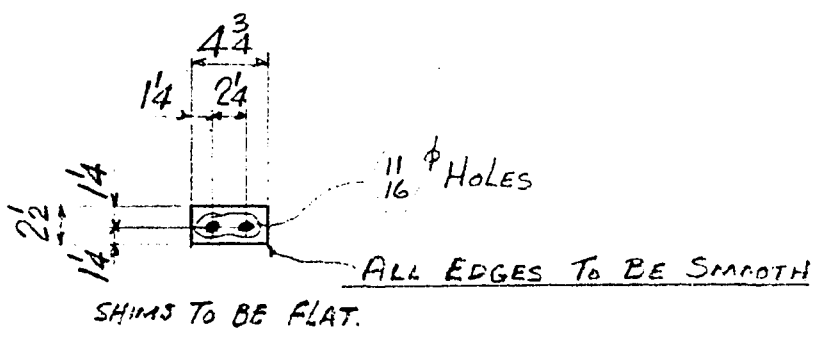


Fig. 4. Detailed Drawing of the Apparatus.

END CONNECT



DOUBLE ANGLE) C1



WIP Bolt)

119

SHIMS EI, FI, GI, HI & KI

NOTE:
- ALL MATERIAL G40.12 UNLESS NOTED

| | | | |
|--|--|--|--|
| | | | |
| | | | |
| | | | |
| | | | |
| | | | |
| | | | |
| | | | |
| | | | |
| | | | |
| | | | |

HOLES 15 ϕ U.N.
 16

BOLTS: 7 ϕ H.S.

SHOP PAINT
NONE
WHEELER RATE ONLY

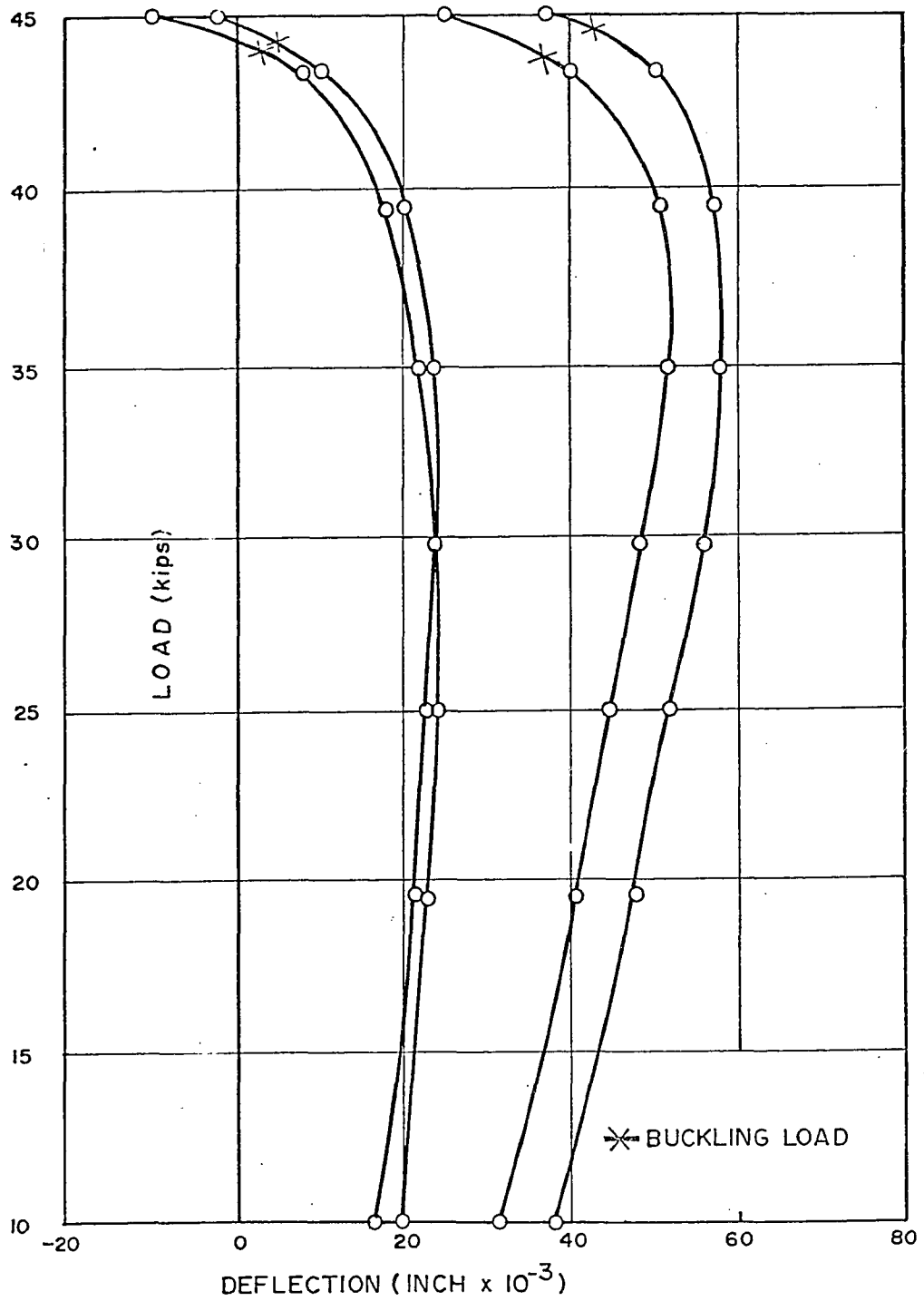


Fig. 5. Buckling load obtained by top-of-the-knee method, for a Single Angle Strut with Hinged ends.

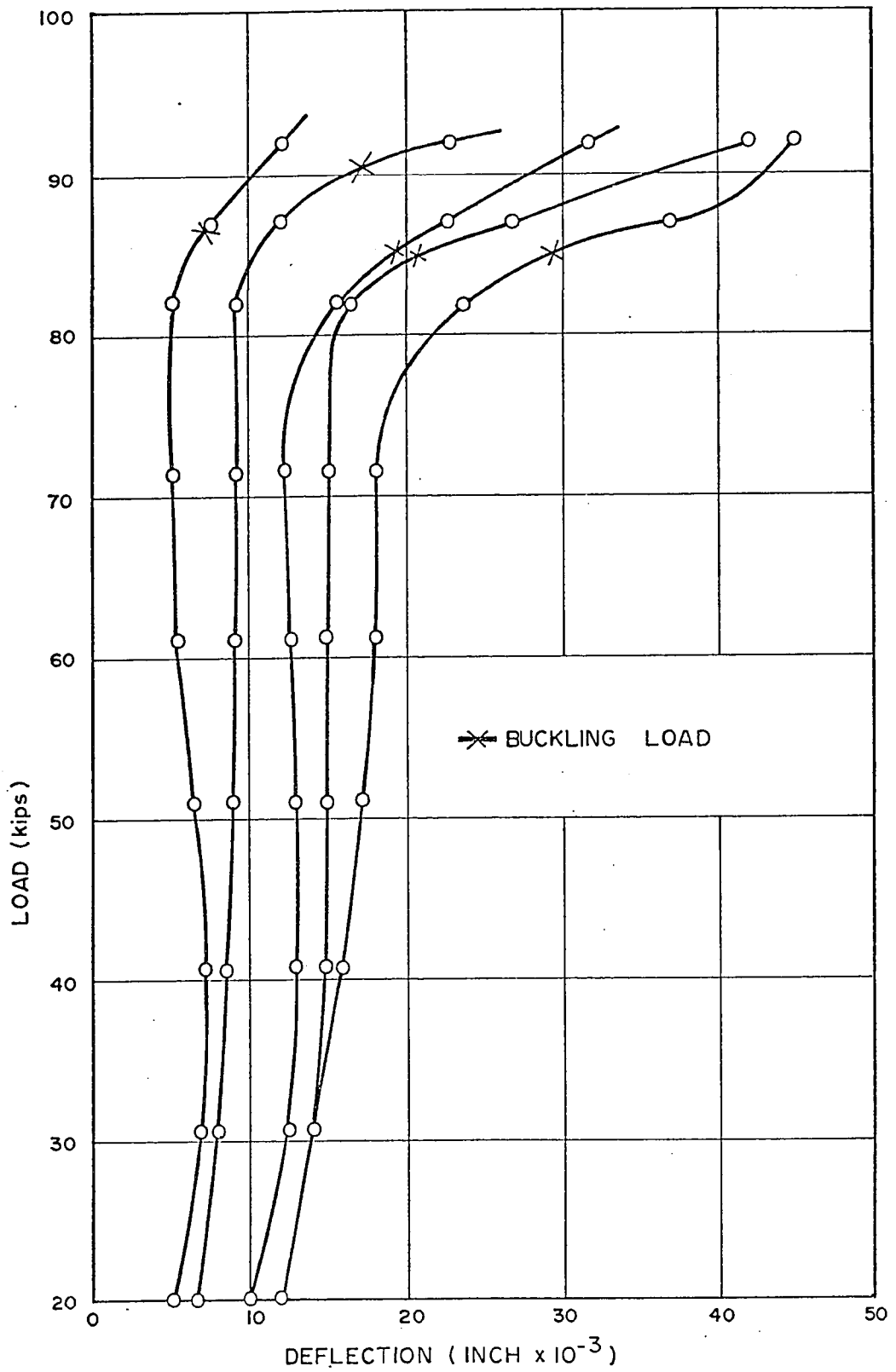


Fig.6. Buckling load obtained by top-of-the-knee method, for a Single Angle Strut with Fixed Ends.

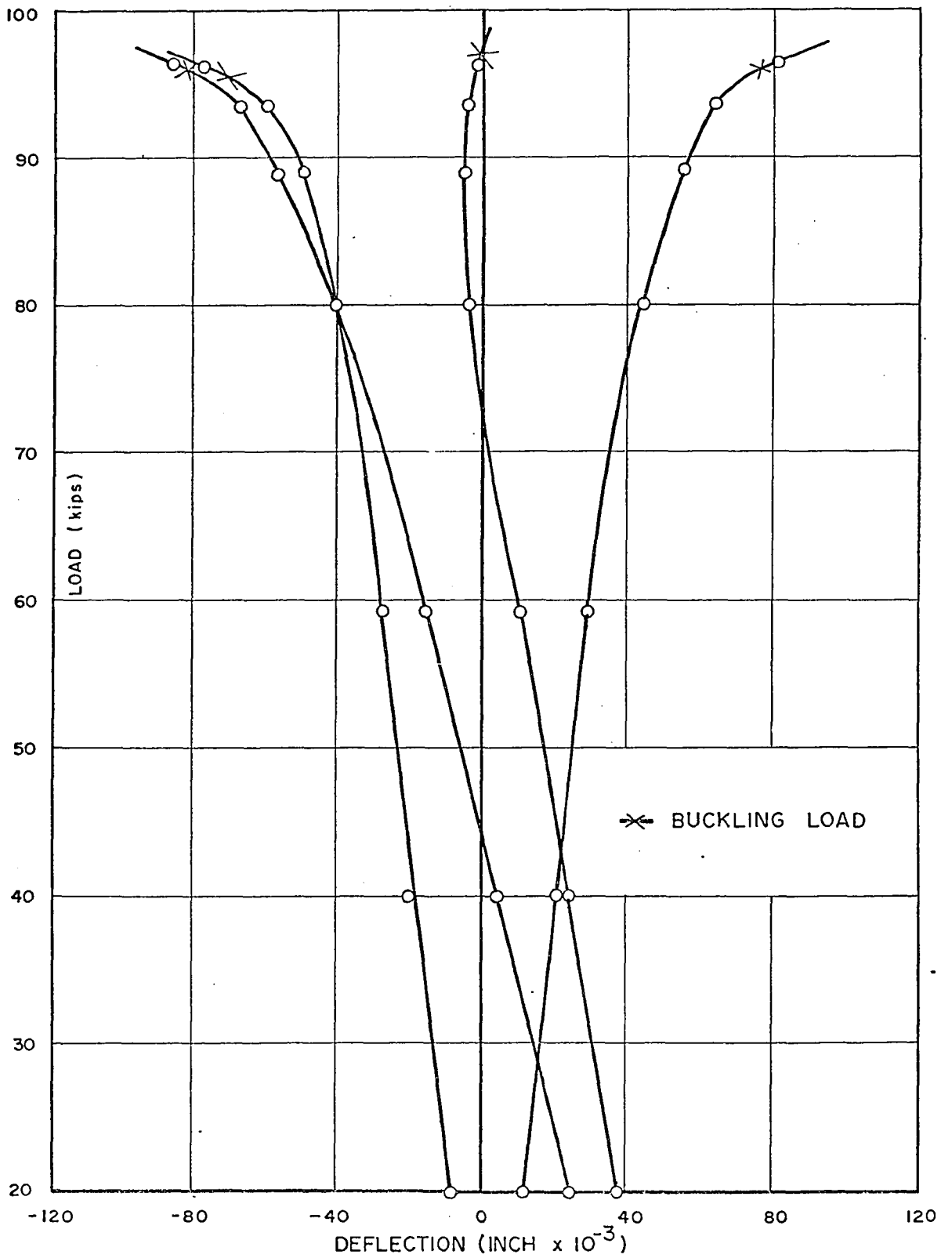


Fig.7. Buckling load obtained by top-of-the-knee method, for a Double Angle strut with Hinged ends.

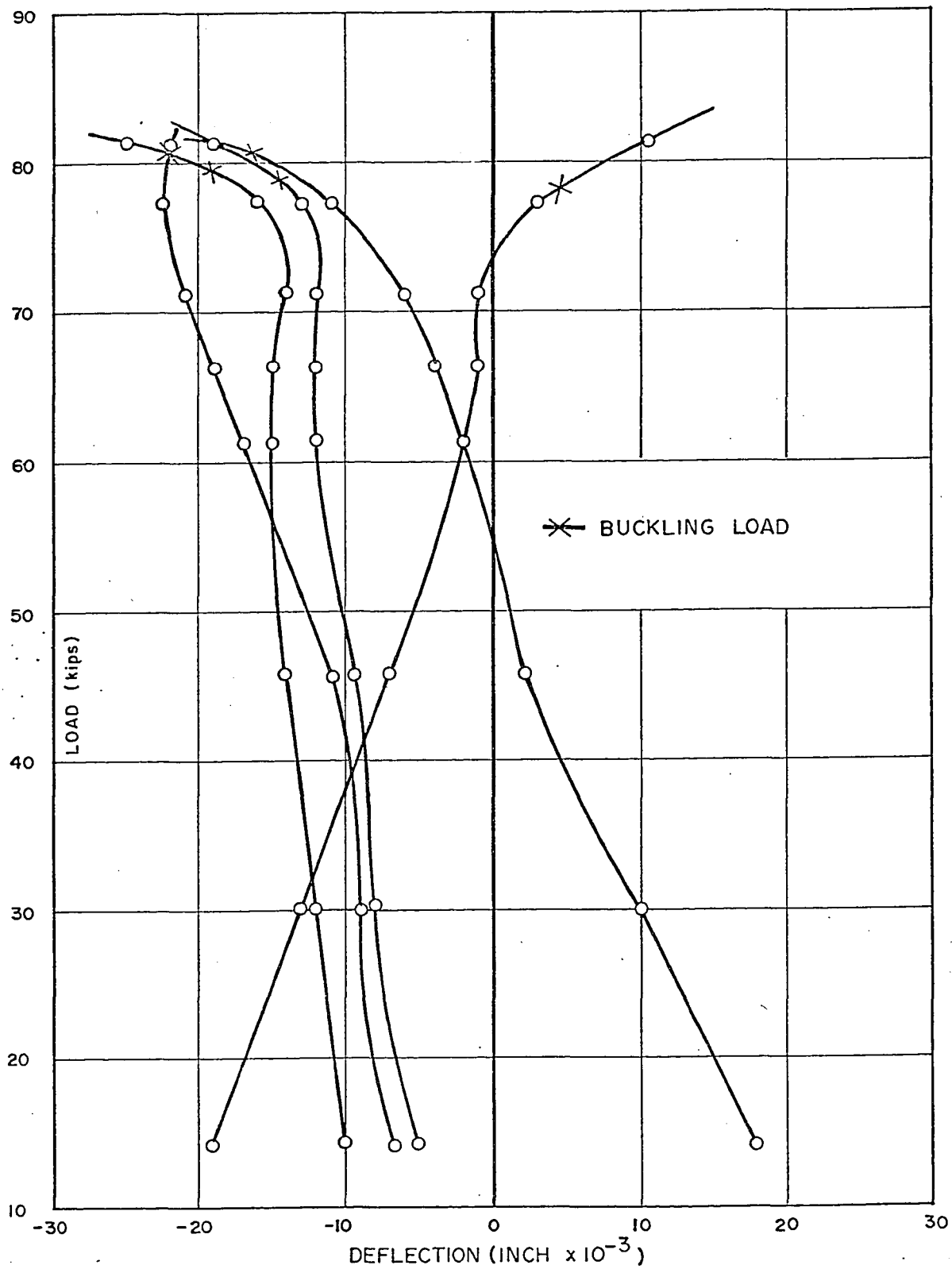


Fig.8. Buckling load obtained by top-of-the-knee method, for a Double Angle with Fixed ends.

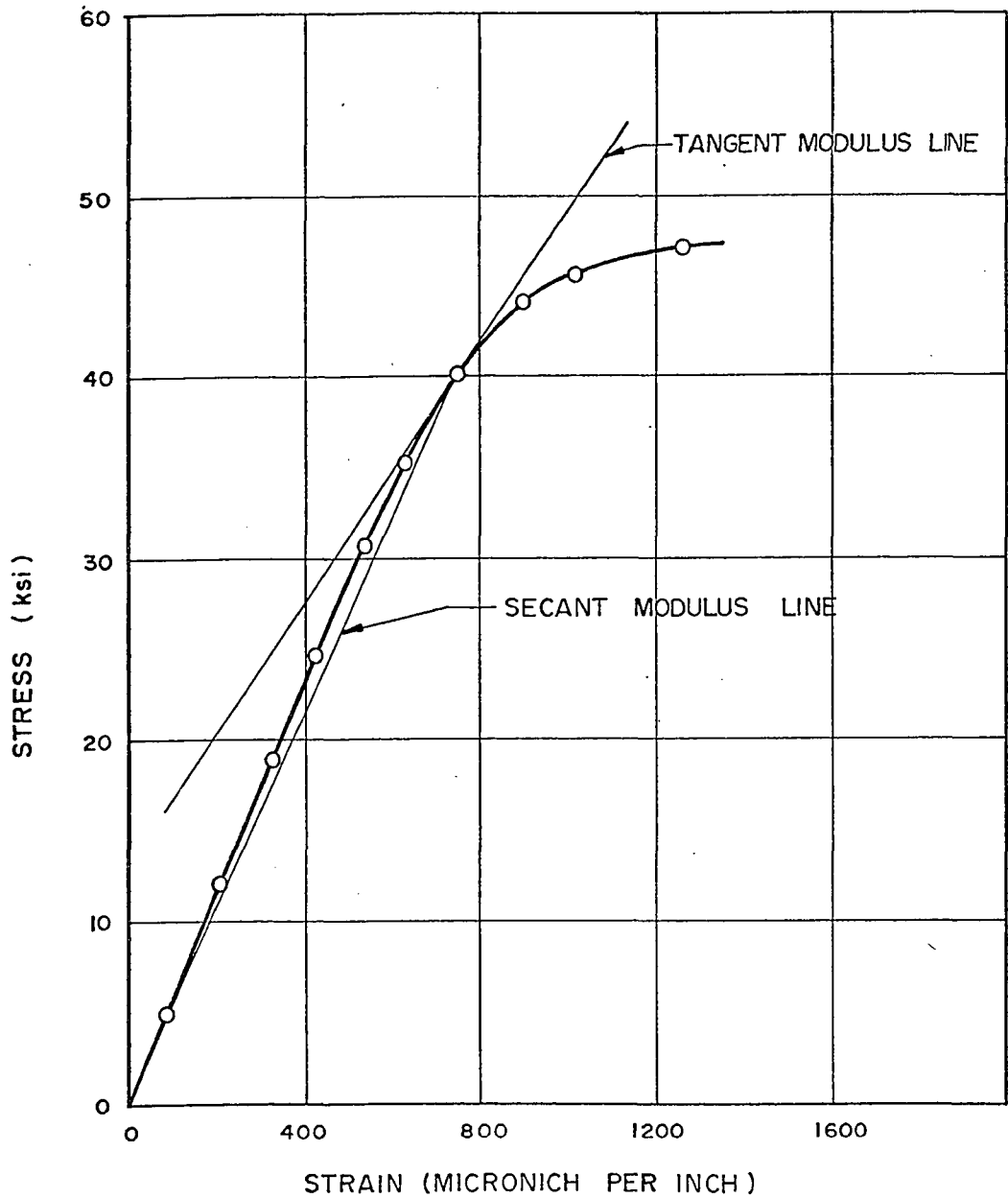


Fig.9. Typical Stress-Strain curve of a Stub Column Test.

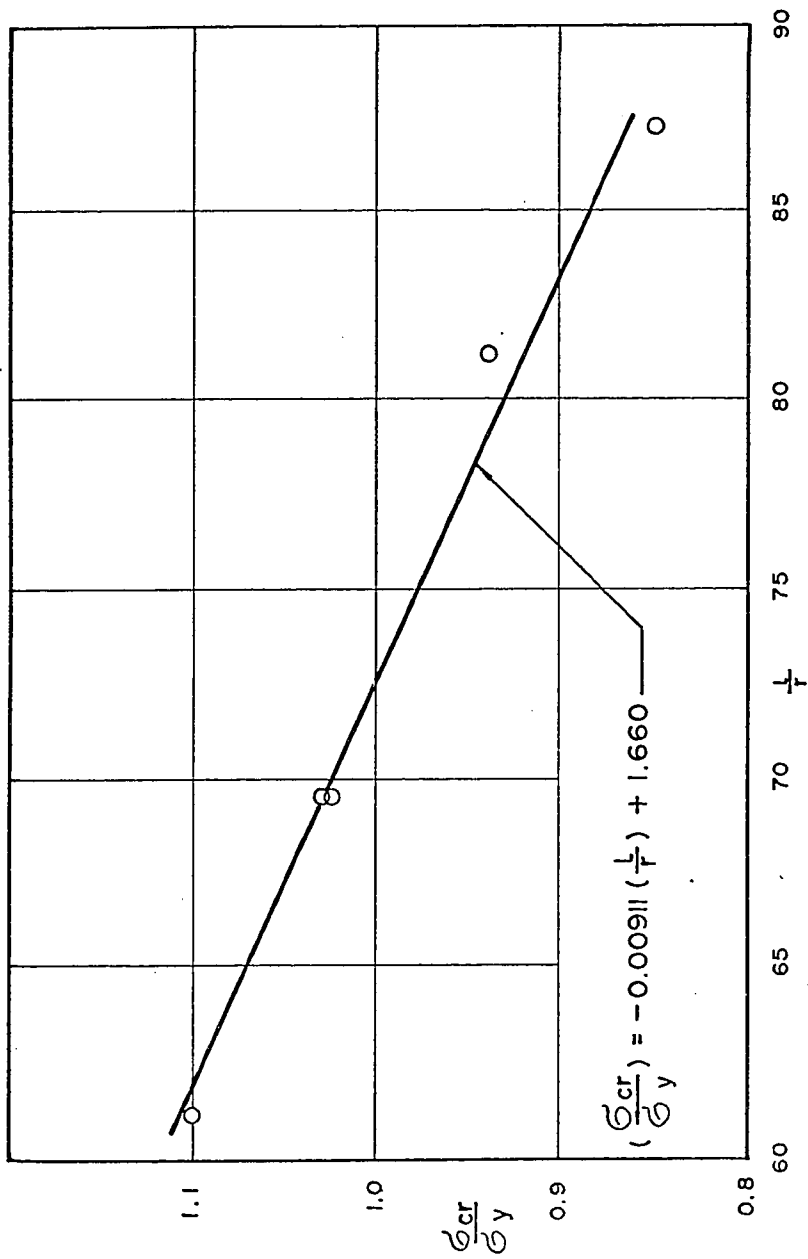
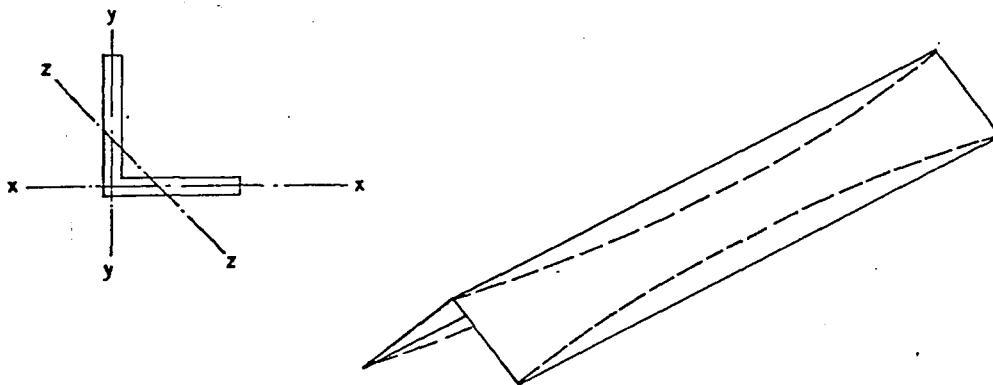
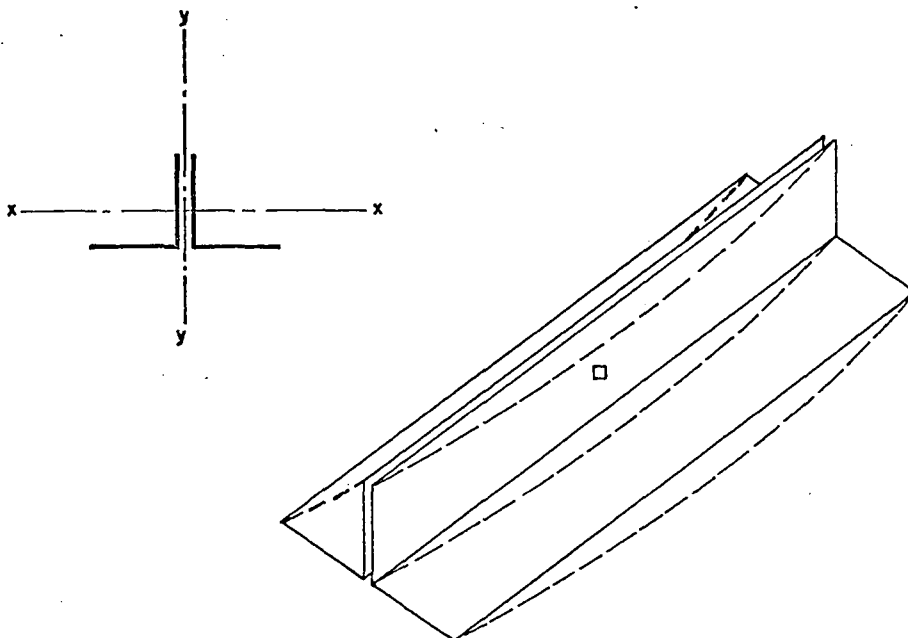


Fig.10. Euler buckling of Single Angle Struts with Hinged Ends.



DOTTED LINE REPRESENTS THE BUCKLED ANGLE

Fig.D11. Euler Buckling of a Single Angle Strut.



DOTTED LINE REPRESENTS BUCKLED DOUBLE ANGLE

Fig.D13. Euler Buckling of a Double Angle strut.

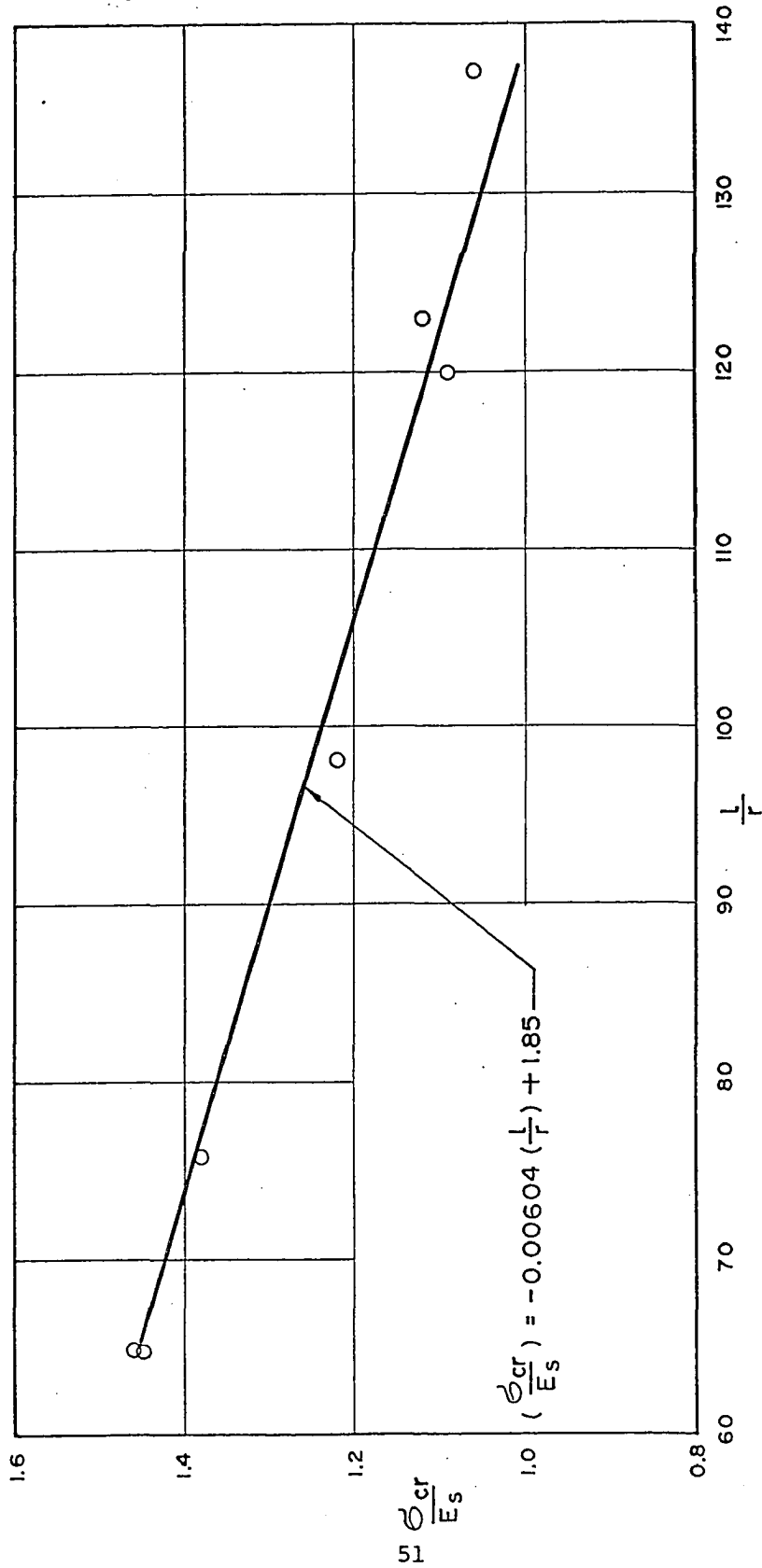


Fig.11. Euler buckling of Single Angle Struts with Fixed Ends.

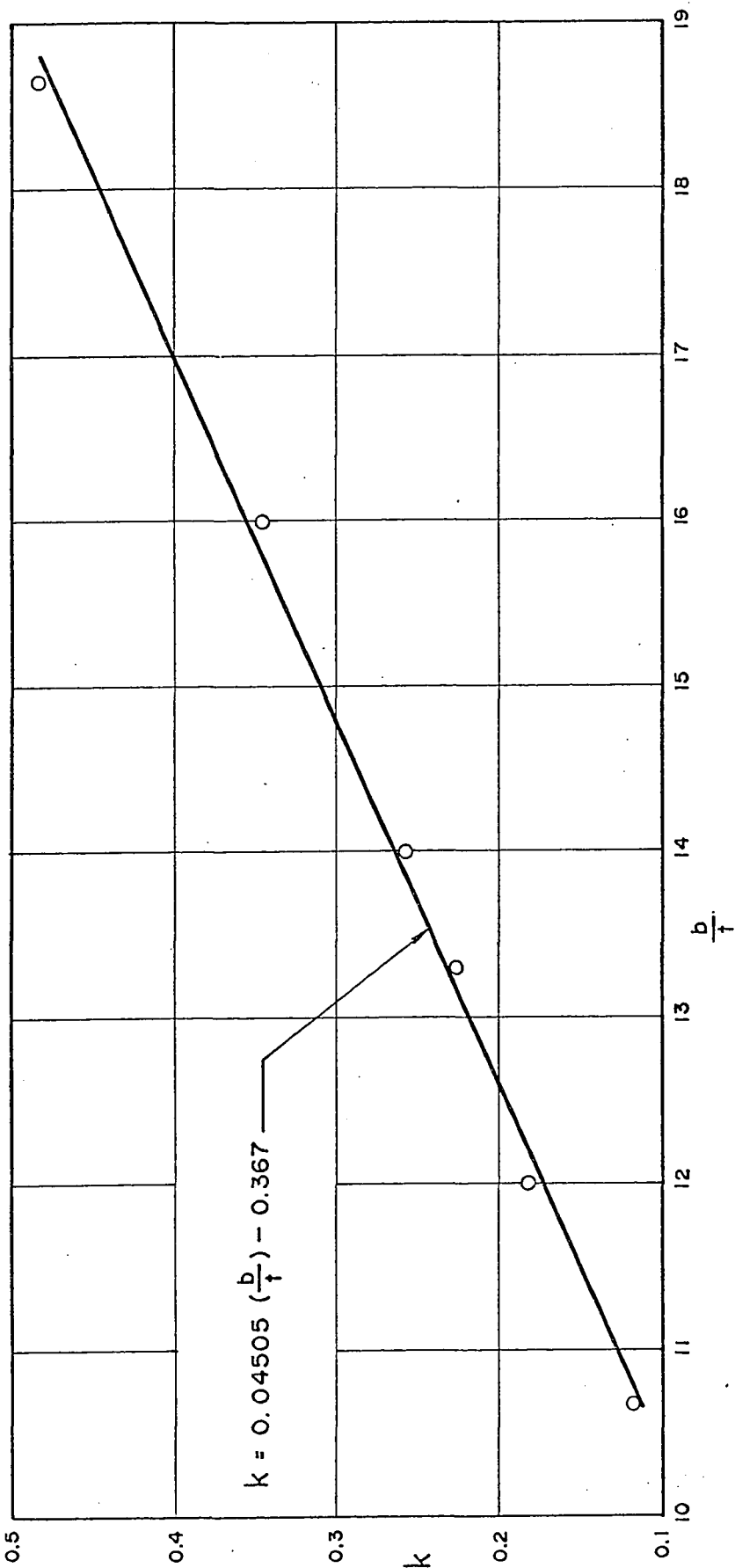


Fig.12. Variation of Plate-coefficient k with b/t ratios of Double Angle Struts --
when tested for Hinged End Conditions.

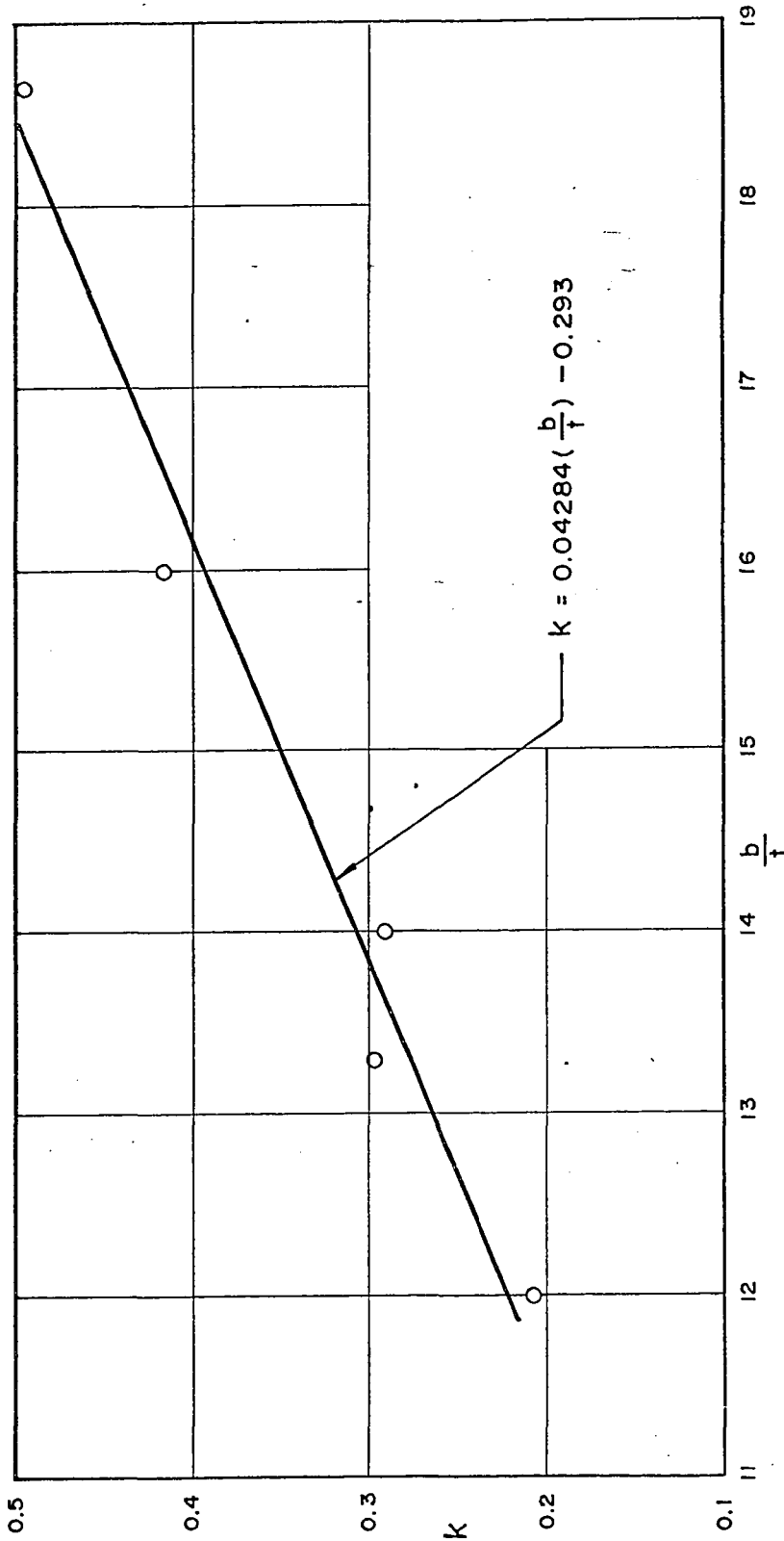


Fig.13. Variation of Plate-coefficient k with b/t ratios of Double Angle Struts --- when tested for Fixed End conditions.

| b/t | Dimensions | l/r | σ_{cr} (Ksi) | σ_p (Ksi) | σ_e (Ksi) | σ_y (Ksi) | σ_{cr}/σ_y | E_s/E |
|-------|----------------|------|------------------------|---------------------|---------------------|---------------------|------------------------|---------|
| 11.20 | 3½ x 3½ x 5/16 | 69.5 | 47.50 | 83.70 | 48.20 | 46.00 | 1.03 | .938 |
| 12.00 | 3 x 3 x 1/4 | 87.2 | 37.28 | 74.00 | 38.10 | 44.00 | 0.85 | .980 |
| 12.80 | 4 x 4 x 5/16 | 60.9 | 39.67 | 60.10 | 40.90 | 36.00 | 1.10 | .900 |
| 14.00 | 3½ x 3½ x 1/4 | 69.5 | 46.00 | 50.80 | 40.80 | 45.85 | 1.025 | .924 |
| 16.00 | 3 x 3 x 3/16 | 81.2 | 39.00 | 38.50 | 33.00 | 41.50 | 0.94 | .934 |
| 18.67 | 3½ x 3½ x 3/16 | 74.7 | 35.08 | 29.90 | 52.50 | 42.50 | 0.828 | .97 |

The yield stress, σ_y is found at an offset of 0.01%.

For angles with $11.2 \leq b/t \leq 18/67$, the relationship $E_s = 0.94E$ may be used.

Table 1. Results of Tests made on Single Angles with Hinged Ends.

| b/t | Dimensions (Inches) | l/r | σ_{cr} (Ksi) | σ_p (Ksi) | σ_e (Ksi) | σ'_{cr}/E_s | E_s/E | K |
|-------|------------------------|------|------------------------|---------------------|---------------------|--------------------|---------|-------|
| 10.67 | 2 x 2 x 3/16 | 123 | 29.75 | 87.00 | 14.10 | 1.12 | .935 | .688 |
| 11.20 | 3½ x 3½ x 5/16 | 64.5 | 40.00 | 79.70 | 39.25 | 1.50 | .916 | .990 |
| 13.30 | 2½ x 2½ x 3/16 | 98.0 | 33.83 | 58.70 | 27.50 | 1.22 | .960 | .904 |
| 14.00 | 3½ x 3½ x 1/4 | 64.5 | 38.30 | 50.35 | 39.60 | 1.46 | .885 | 1.02 |
| 14.00 | 1¼ x 1¼ x 1/8 | 137 | 28.75 | 51.50 | 13.25 | 1.06 | .947 | .680 |
| 16.00 | 3 x 3 x 3/16 | 75.5 | 36.70 | 38.52 | 37.10 | 1.38 | .932 | 1.005 |
| 16.00 | 2 x 2 x 1/8 | 120 | 30.25 | 40.60 | 18.20 | 1.09 | .987 | .775 |
| 18.67 | 3½ x 3½ x 3/16 | 64.5 | 33.25 | 30.90 | 65.20 | 1.16 | .980 | |

For angles with $b > 2$ in. and $b/t \leq 16$, $K = 1$.

For angles with $b \leq 2$ in. and $b/t \leq 16$, $K = 0.714$.

For angles with $10.67 \leq b/t \leq 18.67$, the relationship $E_s = 0.94 E$ may be used.

Table 2. Results of Tests made on Single Angles with Fixed Ends.

| b/t | Dimensions (Inches) | σ_{cr} (Ksi) | k | σ_e (Ksi) | E_s/E |
|-------|------------------------|------------------------|-------|---------------------|---------|
| 10.67 | 2 x 2 x 3/16 | 25.00 | .1160 | 44.10 | .988 |
| 12.00 | 3 x 3 x 1/4 | 31.15 | .1820 | 97.80 | .953 |
| 13.30 | 2½ x 2½ x 3/16 | 32.27 | .2260 | 70.00 | .982 |
| 14.00 | 1¾ x 1¾ x 1/8 | 31.73 | .2575 | 30.90 | .950 |
| 16.00 | 2 x 2 x 1/8 | 35.00 | .3440 | 46.50 | .963 |
| 18.67 | 3½ x 3½ x 3/16 | 34.27 | .4825 | 130.0 | .953 |

For angles with $10.67 \leq b/t \leq 18.67$, the relationship

$E_s = 0.965E$ may be used.

Table 3. Results of Tests made on Double Angles with Hinged Ends.

| b/t | Dimensions (Inches) | σ_{cr} (Ksi) | k | σ_e (Ksi) | E_s/E |
|-------|------------------------|------------------------|-------|---------------------|---------|
| 10.67 | 2 x 2 x 3/16 | 40.67 | .2400 | 14.00 | |
| 12.00 | 3 x 3 x 1/4 | 35.40 | .2060 | 104.0 | .950 |
| 13.30 | 2½ x 2½ x 3/16 | 40.27 | .2990 | 62.00 | .950 |
| 14.00 | 1¾ x 1¾ x 1/8 | 37.53 | .2900 | 35.80 | .987 |
| 16.00 | 2 x 2 x 1/8 | 39.47 | .4150 | 45.00 | .958 |
| 18.67 | 3½ x 3½ x 3/16 | 35.83 | .4940 | 142.0 | .980 |

σ_e was calculated using constant $K = 1$, in Euler formula (22)

For angles with $10.67 < b/t \leq 18.67$, the relationship

$E_s = 0.965E$ may be used.

Table 4. Results of Tests made on Double Angles with Fixed Ends.

| b/t | Dimensions (Inches) | σ_{cr} (Ksi) | Remarks |
|-----|------------------------|------------------------|--|
| 16 | 2 x 2 x 1/8 | 37.75 | No connecting bolts used. Tests made with hinged ends. |
| 16 | 2 x 2 x 1/8 | 40.75 | No connecting bolts used. Tests made with fixed ends. |
| 16 | 2 x 2 x 1/8 | 33.50 | Three connecting bolts used. Tests made with hinged ends. |
| 16 | 2 x 2 x 1/8 | 47.25 | Three connecting bolts used. Tests made with fixed ends. |

Table 5. Results of Tests made on Double Angles with varying number of Connecting bolts.

| Item | Quantity | Shape | Dimensions (Inches) | Length |
|------------------|----------|----------|------------------------|-----------------|
| 110 | 2 | Channel | 12 @ 20.7 | 9ft. 7½in. |
| 111 ^R | 2 | Channel | 12 @ 20.7 | 6-3/4in. |
| 111 ^L | 2 | Channel | 12 @ 20.7 | 6-3/4in. |
| 112 | 4 | Angle | 6x4x3/4 | 1ft. 8in. |
| 113 | 3 | Plate | 9x3/8 | 1ft. 8in. |
| 114 | 2 | Plate | 13-3/4x3/4 | 1ft. 8in. |
| 115 | 1 | Plate | 20x1/4 | 8ft. 4in. |
| 116 | 1 | W.Flange | 6 @ 15 | 9in. |
| 117 | 1 | Plate | 11-15/16x1-1/2 | 1ft. 1-15/16in. |
| 118 | 1 | Plate | 11-15/16x1-1/2 | 1ft. 1-15/16in. |
| 119 | 1 | Plate | 11x1-1/2 | 1ft. |
| 120 | 1 | Plate | 6-3/4x1/4 | 9-1/2in. |
| 121 ^R | 1 | Angle | 5x3-1/2x3/8 | 4-3/4in. |
| 121 ^L | 1 | Angle | 5x3-1/2x3/8 | 4-3/4in. |
| E 1 | 4 | Plate | 2-1/2x1/32 | 4-3/4in. |
| F 1 | 4 | Plate | 2-1/2x1/16 | 4-3/4in. |
| G 1 | 4 | Plate | 2-1/2x1/8 | 4-3/4in. |
| H 1 | 4 | Plate | 2-1/2x1/4 | 4-3/4in. |
| K 1 | 4 | Plate | 2-1/2x1/2 | 4-3/4in. |

Table 6. Details of Members shown in fig. 4.

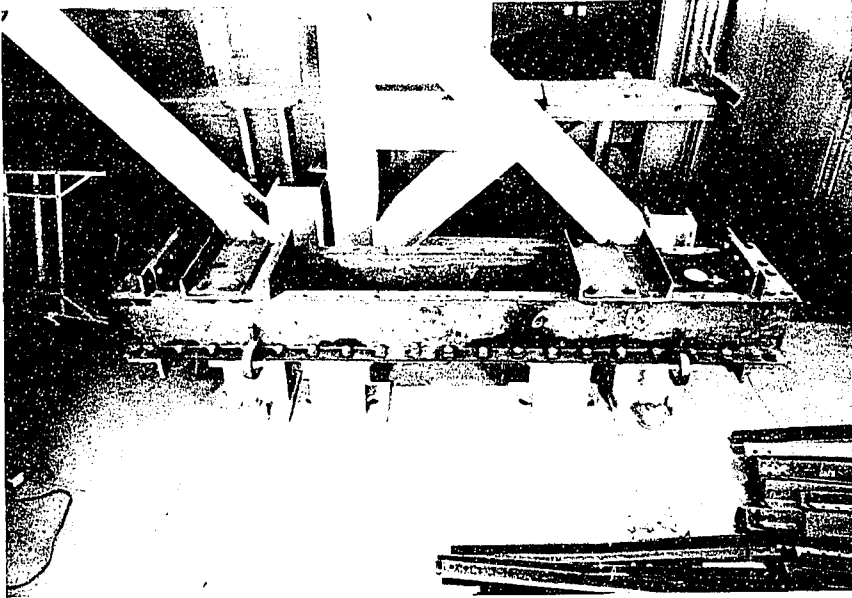


Photo 1(a). Lay-out of Test Apparatus.

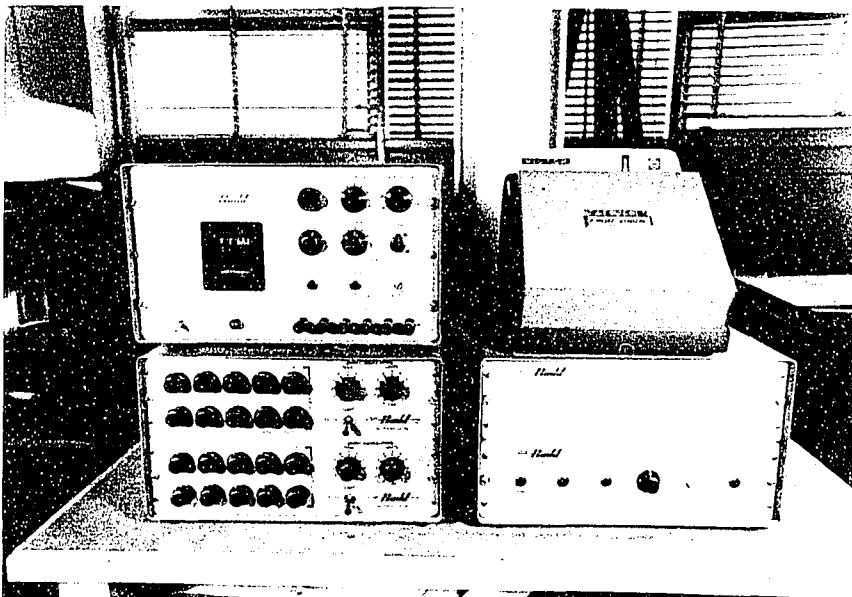


Photo 1(b). Datran Strain Reader.

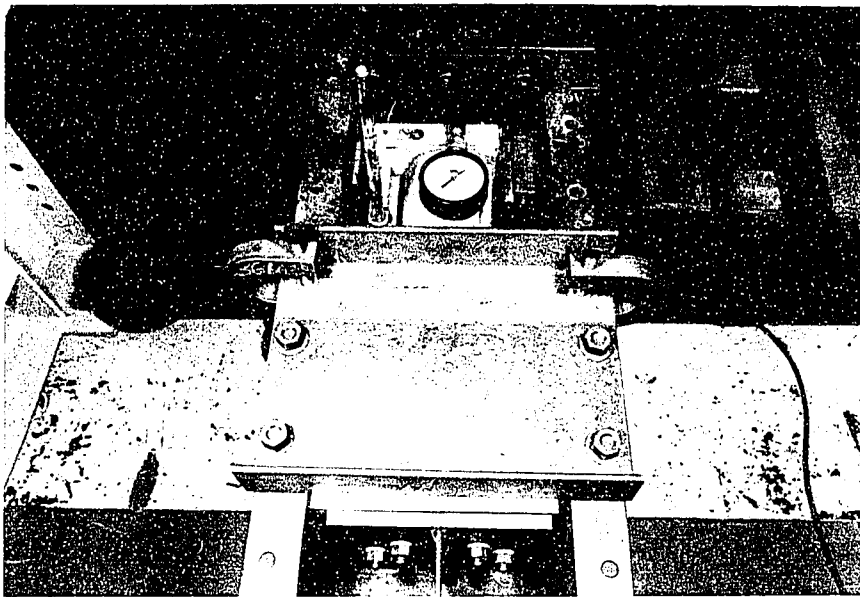
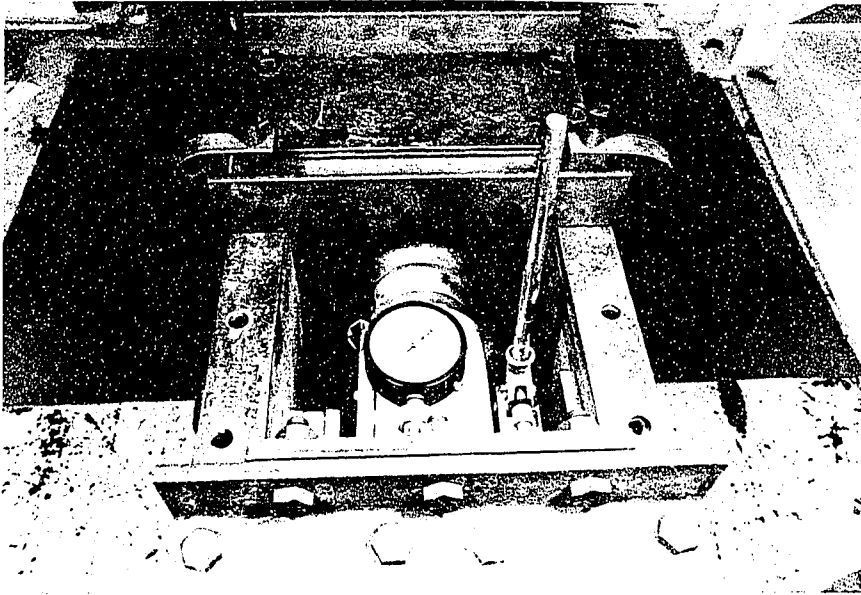


Photo 2. Two Views of the Loading Arrangement.

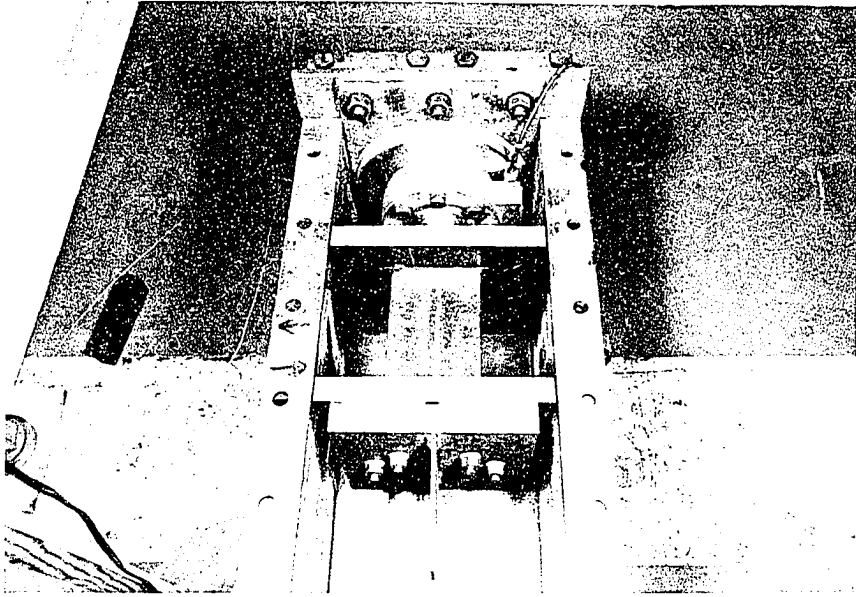


Photo 3(a). View of 'Load Cell end' with Batten plate removed.

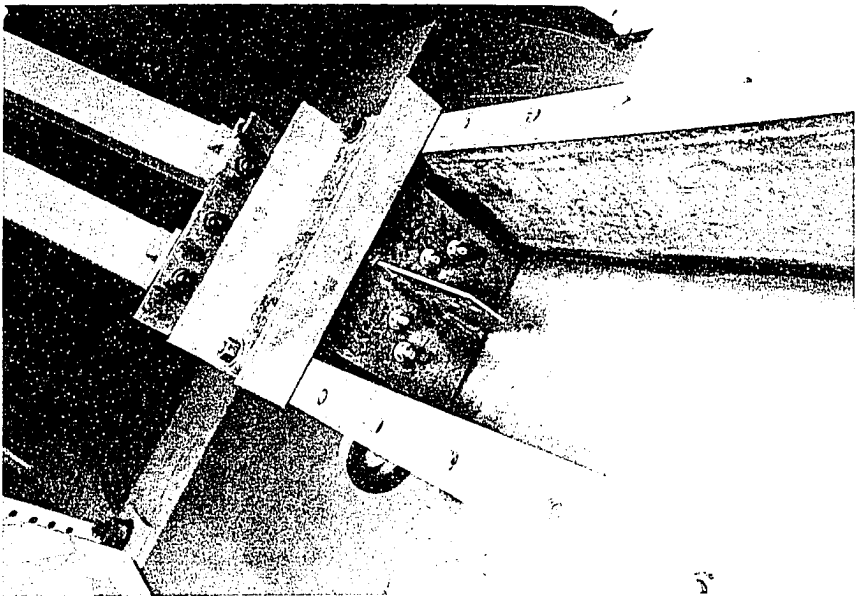


Photo 3(b). View of "Load Cell End" with Batten plate in position.

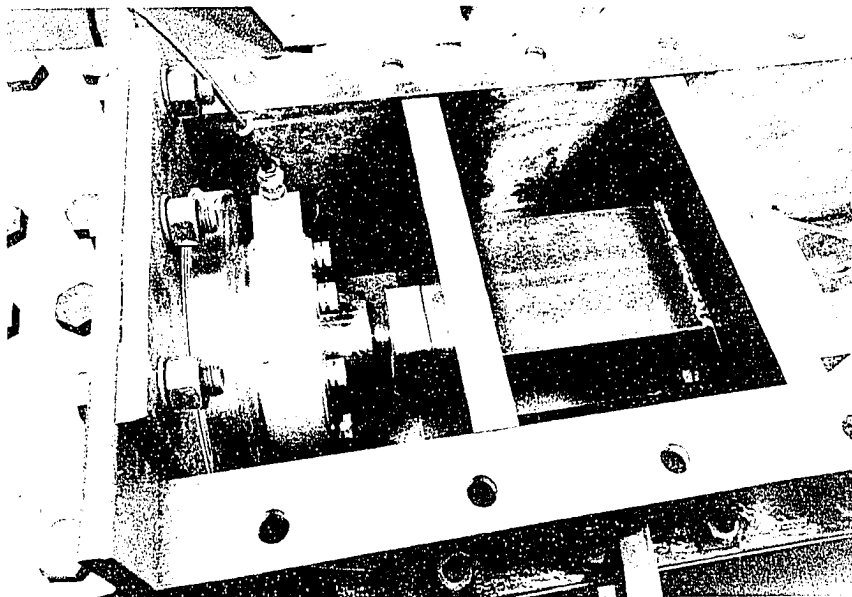


Photo 4. View of Load Cell.

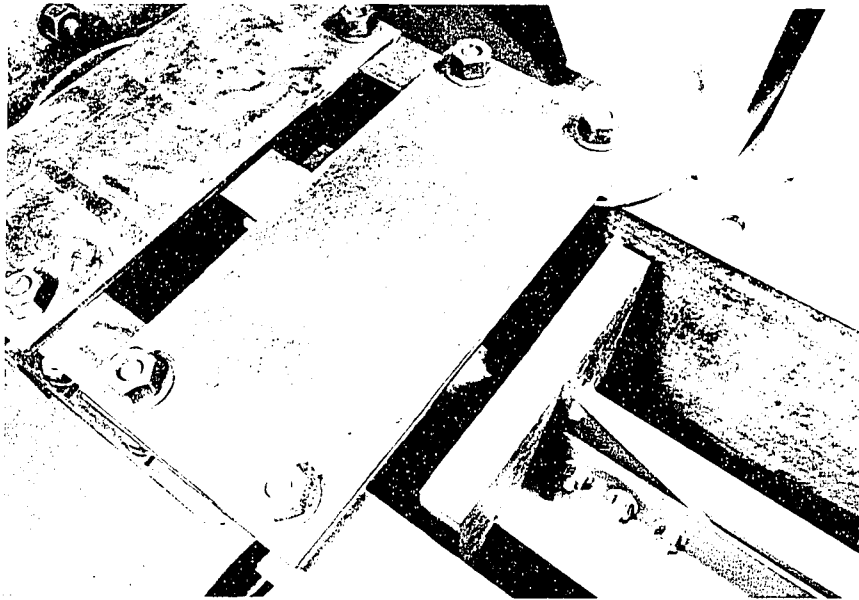
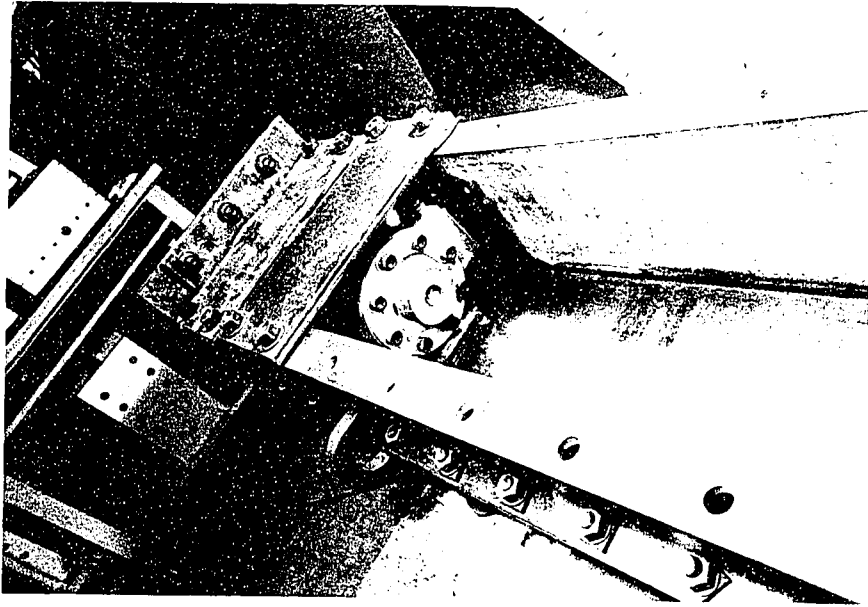


Photo 5. Two Views of the Hinged End Arrangement at the 'Load Cell End'..

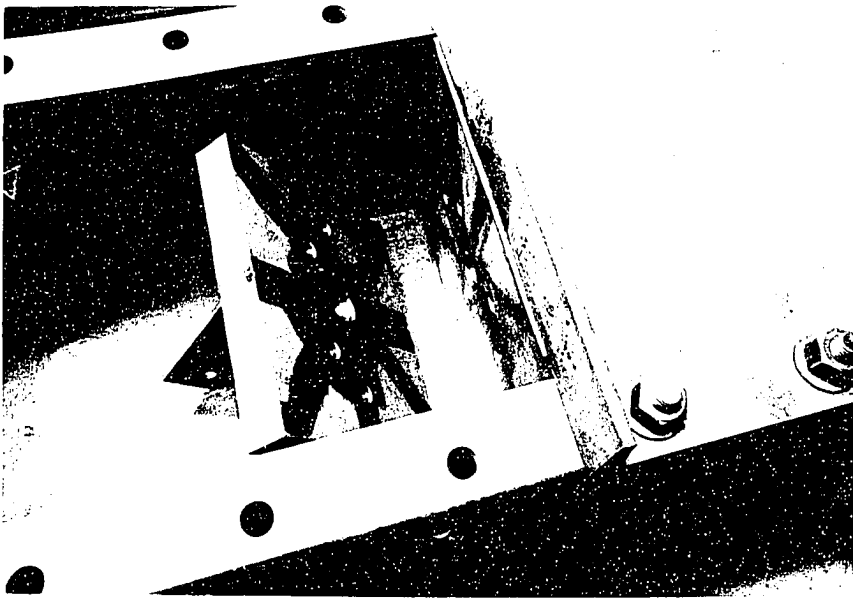
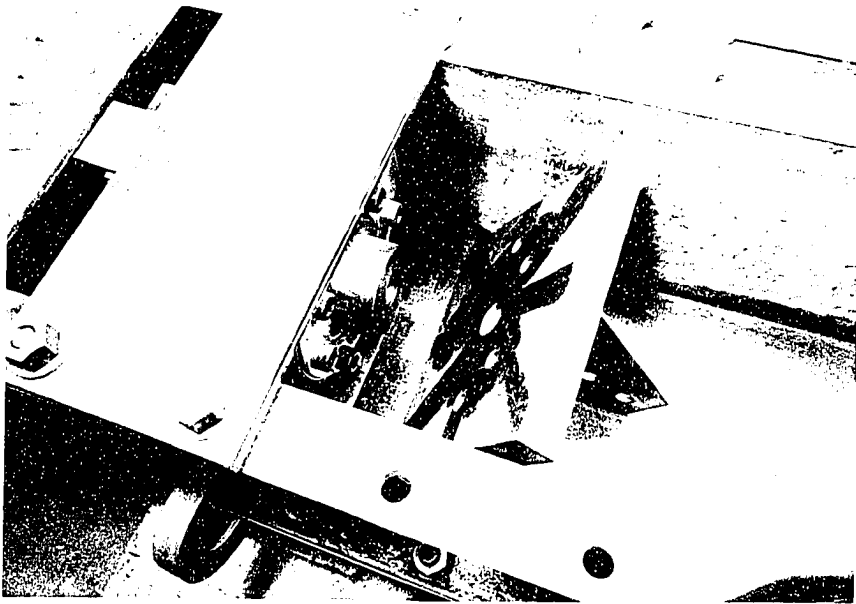


Photo 6. Views of the two Hinged Ends.

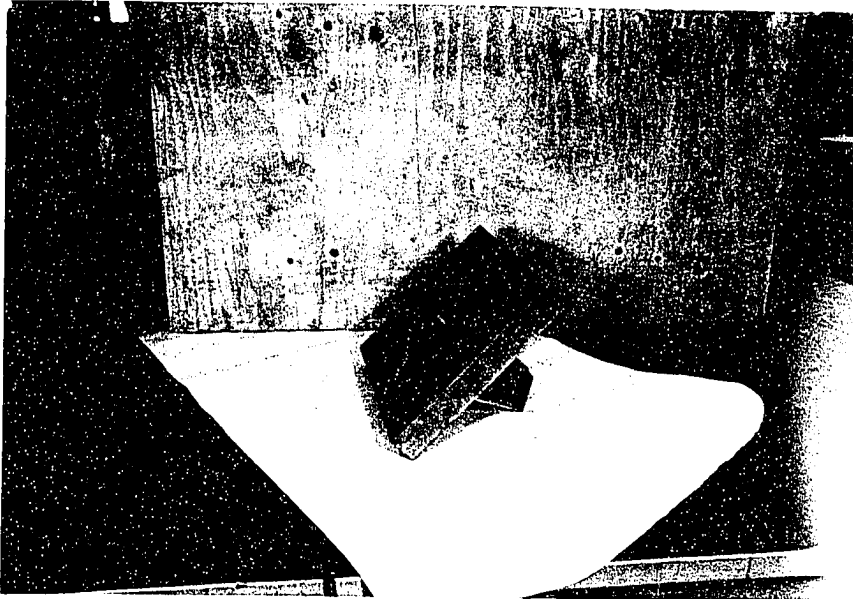
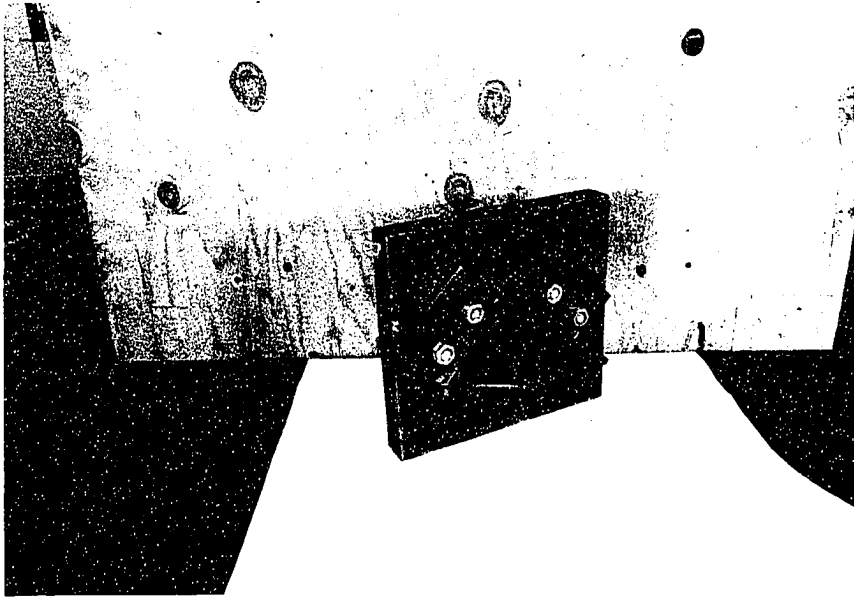


Photo 7. "End Connections for Single Angles."

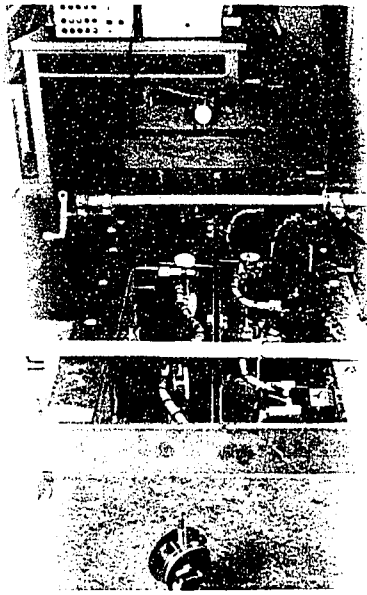


Photo 8(a). Set-up before commencing a Test.

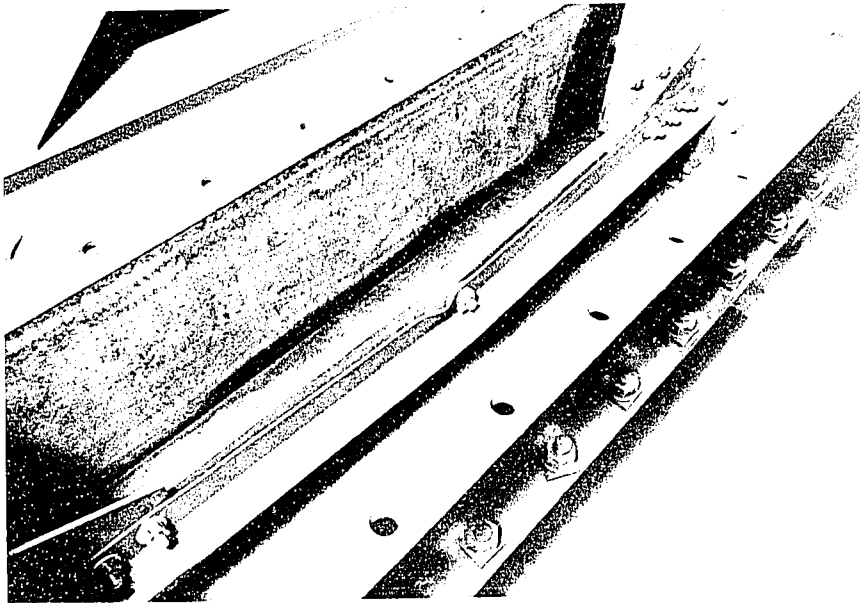


Photo 8(b). View after the Experiment.

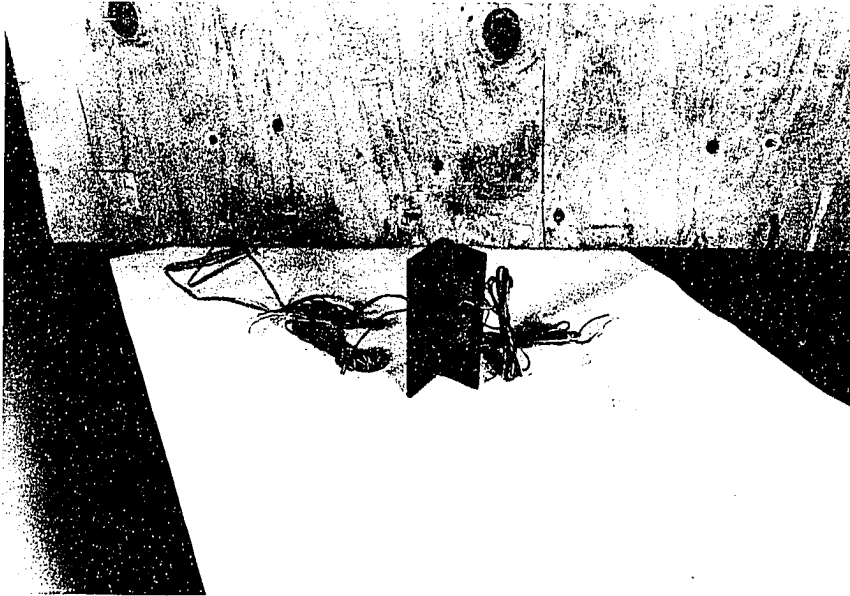


Photo 9. Stub Columns .

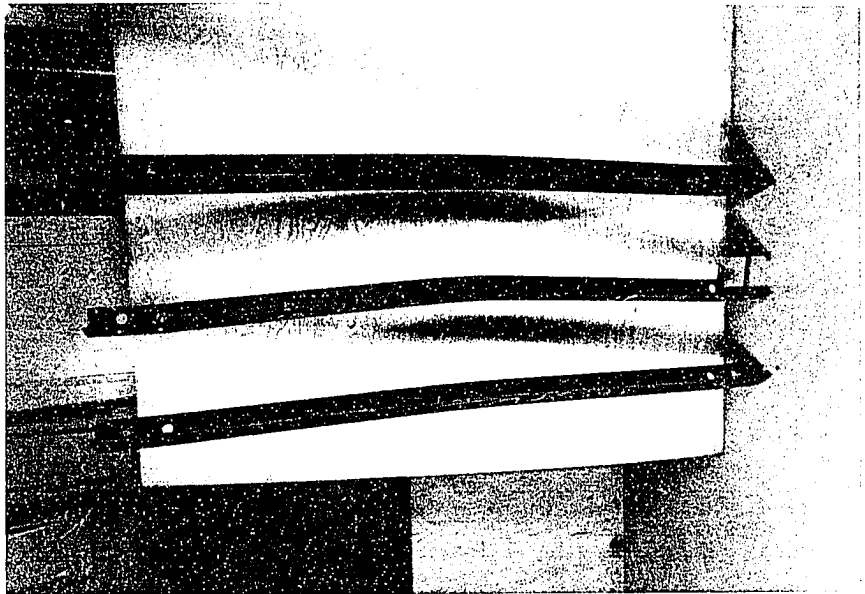
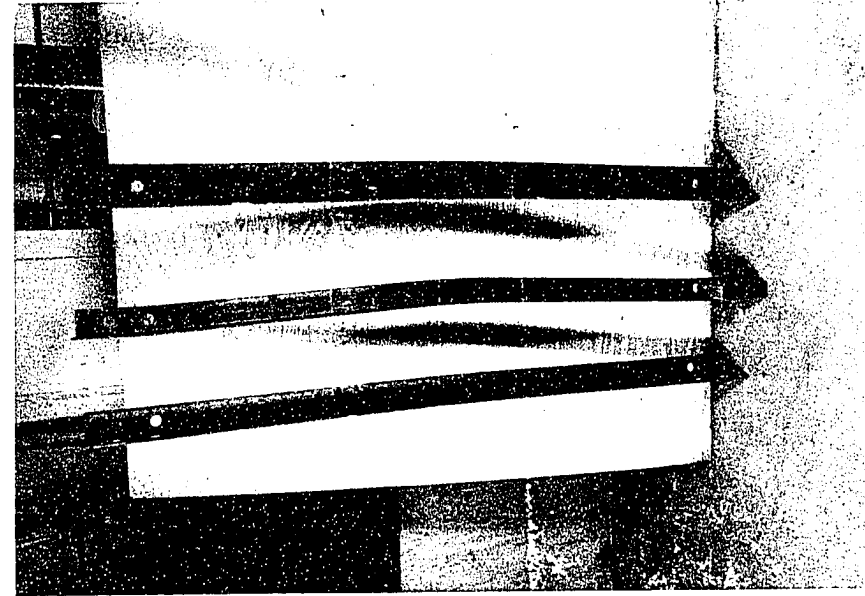


Photo 10. Buckled forms of Single Angles due to Euler Buckling.

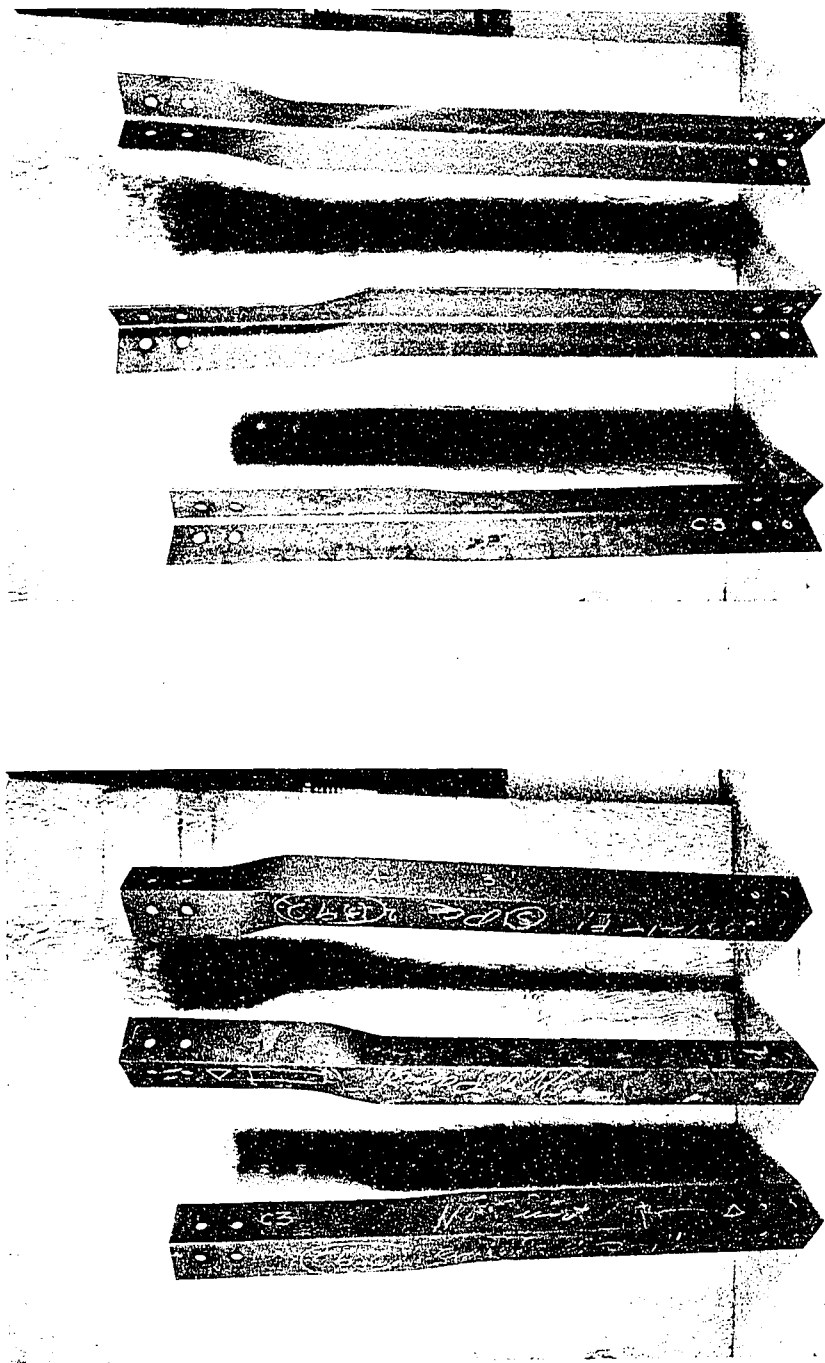


Photo 11. Buckled forms of Single Angles due to Local Buckling.

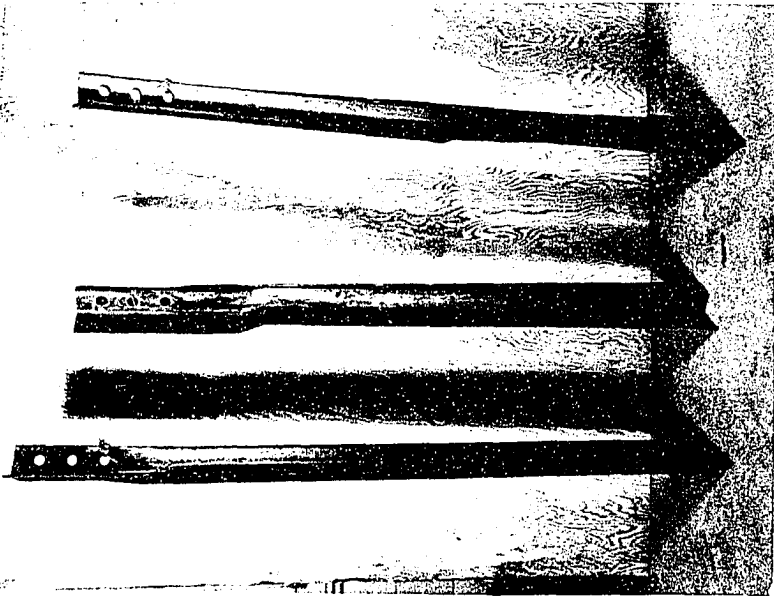
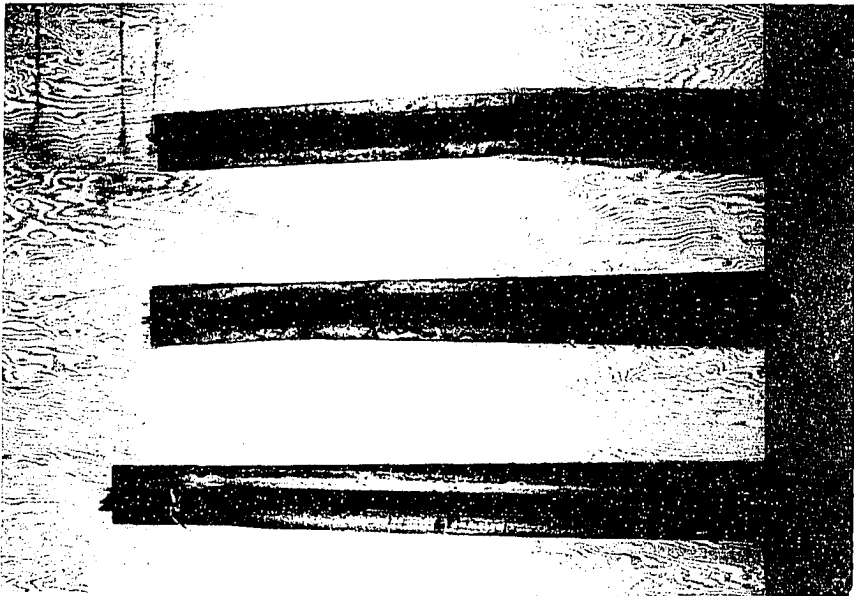


Photo 12. Buckled forms of Double Angles (with no connecting bolts) - Local Buckling.

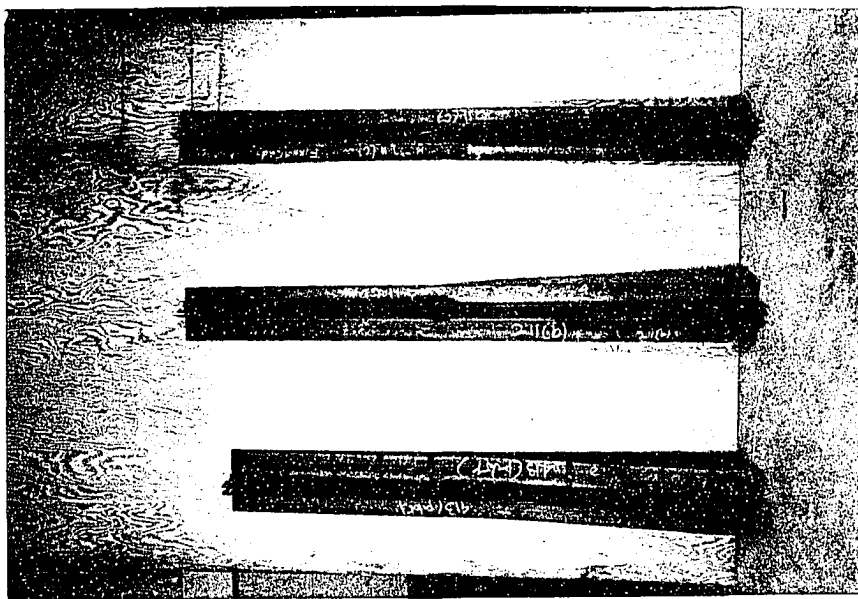
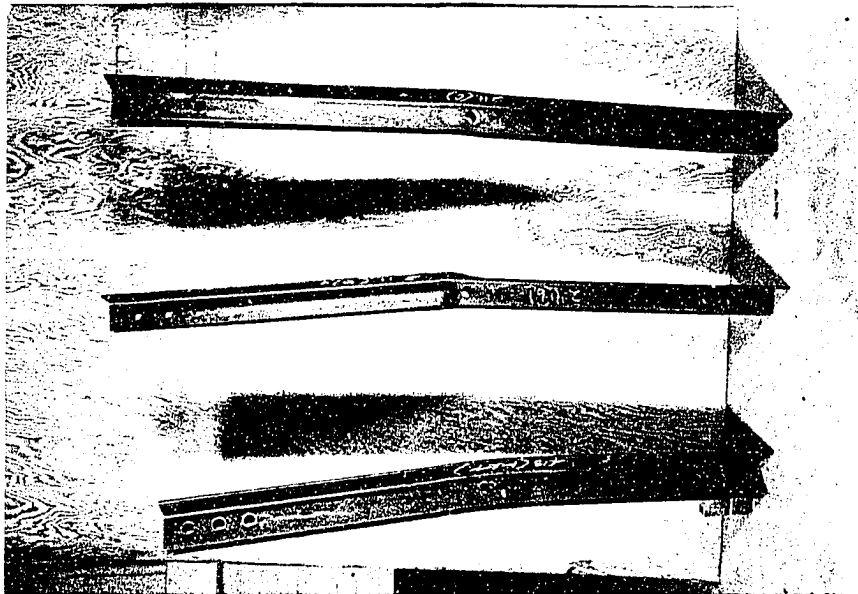


Photo 13. Buckled forms of Double Angles (with one connecting bolt) - Local Buckling.

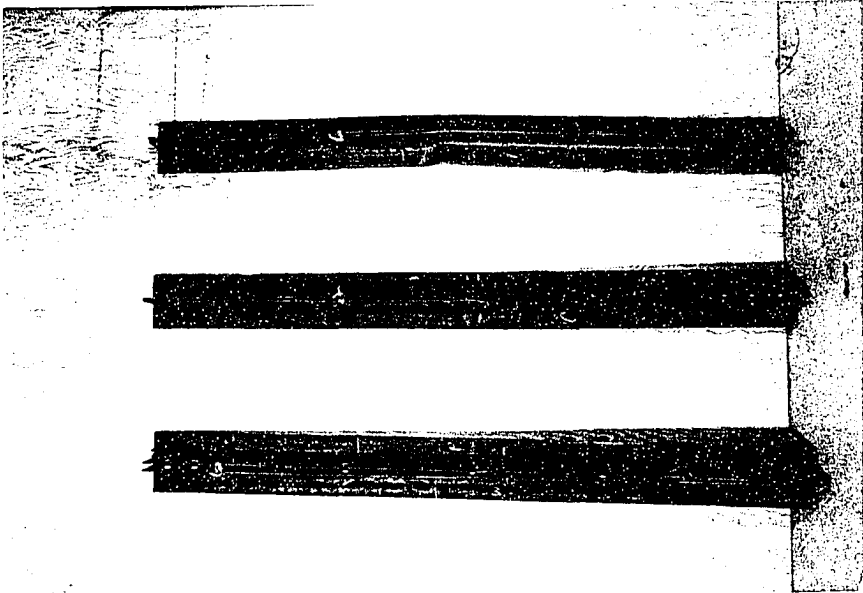
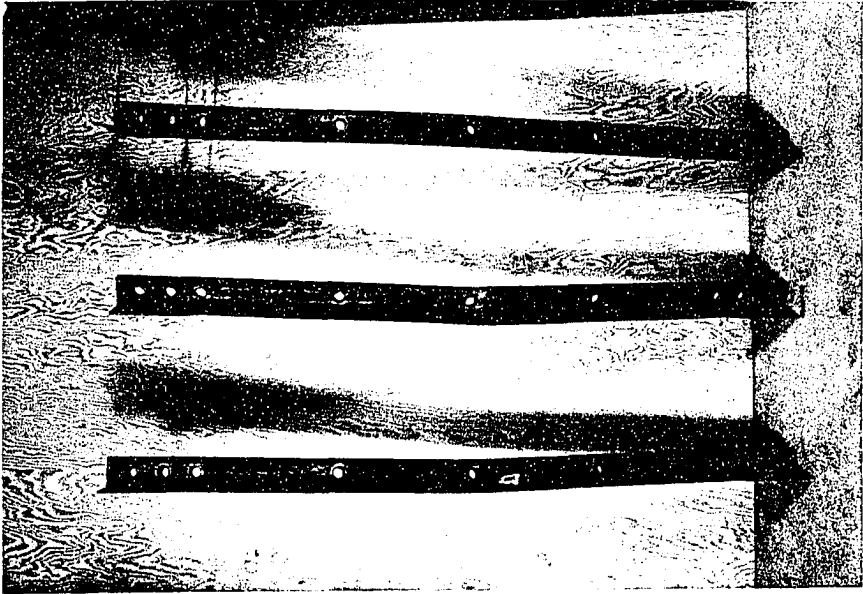


Photo 14. Buckled forms of Double Angles (with three connecting bolts) - Local Buckling.

VITA AUCTORIS

- 1942 Born November 13, Nairobi, Kenya.
- 1962 Passed Cambridge Higher School Certificate Exam.
 at the Duke of Gloucester School, Nairobi.
- 1966 Graduated from the University of London with a
 Bachelor of Science Degree in Civil Engineering.
- 1966 September, Employed by Sir William Arrol & Co.,
 Glasgow, Scotland.
- 1967 September, Joined the University of Windsor to
 study for a Masters Degree in Civil Engineering.